SUPPORTING INFORMATION (SI)

Lipophilic ferulic acid derivatives protect PC12 cells against oxidative damage via modulating *β*-Amyloid aggregation and activating Nrf2 enzymes

Yu Wu,†[a] Yu-gang Shi,†*[a] Xiao-liang Zheng,[b] Ya-li Dang,[c] Chen-min Zhu,[a] Run-run Zhang,[a] Yu-ying Fu,[a] Tian-yi Zhou,[b] Jun-hui Li[d]

[a]*School of Food Science and Biotechnology, Zhejiang Gongshang University, Hangzhou, Zhejiang 310035, China*

[b]*Center for Molecular Medicine, Zhejiang Academy of Medical Sciences, Hangzhou 310013, China; Hangzhou*

[c]*Key Laboratory of Animal Protein Food Processing Technology of Zhejiang Province, Ningbo University, Ningbo 315211, China*

[d]*Zhejiang Key Laboratory for Agro-Food Processing, Department of Food Science and Nutrition, Zhejiang University, Hangzhou 310058, China*

Corresponding Author:

Dr. Yu-gang Shi

School of Food Science and Biotechnology, Zhejiang Gongshang University, Xiasha University Town, Xuezheng Str. 18, Hangzhou 310018, China

Tel.: 86–0571–28008927

General conditions for the alcoholysis to prepare FAEs

Ferulate esters with different direct chain fatty alcohols (1-butanol, 1-hexanol, 1-octanol, 1-decanol, and 1-laurinol) were synthesized as described by Shi et al (2017, 2018). The alcoholysis reactions of MF with these fatty alcohols were conducted in a 30 mL glass vial equipped with a tight screw-cap. MF and fatty alcohols (molar ratio, 1:6) were added to 10 mL DES with water (10%, w/w). The reaction was initiated by adding 10 mg of crushed CalB immo Plus. All experiments were carried out under sonochemical irradiation of 150 W, at 50 ^{o}C, for an hour, and subsequently, the reaction bottles were incubated in an orbital shaker at 200 rpm at 60 ^{o}C up to 7 days. The supernatants were analyzed by TLC on Silica gel 60F254 aluminum sheets (0.2 mm thickness, Merck) and high-performance liquid chromatography (HPLC) using a Waters pump (Waters 1525). The conversion of MF into products was calculated as the area percentage of the product peak against the total areas of the substrate (MF) and product peaks. After the completion of the reaction, any solid including lipase was removed by centrifugation and lipase was washed thoroughly with hexane for the reuse. Evaporation of the solvent gave a product mixture, which was separated by silica gel column chromatography using hexane/ethyl acetate (96:4, v/v) as the eluent and/or crystallization

HPLC analysis

HPLC conditions were as follows: Welchrom-C18 column (250 mm×4.6 mm, 5 μm particle size, Welch Materials, MD, USA), equipped with an auto-sampler (model G7129A), and an ultraviolet diode-array (UV-DAD) detector (UV6000LP), Methanol-

phosphoric acid 3 mM (95: 5) as mobile phase (flowrate: 0.75 mL/min), and column temperature of 35 ^{o}C. Peak integration was then performed by using ChemStation Edition software (LC-02).

Cell Viability Assay

Cell viability was assessed by measuring the metabolism of MTT. Briefly, cells were plated in 96-well cell culture plates in 100 μL (1×10^4 cells/well) and pretreated with various concentrations of FA and its alkyl esters (10, 50, and 100 μmol/L) for 24 h. Thereafter, to each well was added MTT solution (20 μL/well) with the final concentration of 5 mg/mL. After 4 h at 37 ^{o}C, the supernatant was discarded and MTT crystals were dissolved in 150 μL of dimethyl sulfoxide. The absorbance of samples was measured at 490 nm with a multimode microplate reader (Synergy2, Bio-Tek, WI, USA). For relative quantification, the value of absorbance in each group was normalized to that in the control group.

Aβ_{1-42} Aggregation Inhibition Activity Assay

The A$\beta_{1–42}$ aggregation inhibition assay was carried out based on the thioflavin T fluorescence method with some modification (Li et al., 2017). A$\beta_{1–42}$ stock solution (1 mM, dissolved in DMSO) was incubated in an ultrasonic bath for 30 min and diluted with phosphate buffer saline (10 mM, pH 7.4). Then the peptide solution (final Aβ concentration of 40 μM) was incubated at 37 °C for 72 h with test compounds (in 1 μM, 5 μM, 10 μM, 50 μM, and 100 μM concentration). Afterward, 80 μL of test solution was diluted to 600 μL with a phosphate buffer containing 10 μM thioflavin T, the fluorescence intensity against the blank (10 μM thioflavin T solution) was recorded. Then,

the fluorescence intensity was performed with multimode microplate reader (SpectraMax M4, Molecular Devices, Sunnyvale, CA, USA) (λexc=450 nm/λem=485 nm). Aggregation inhibition attributed to the presence of the extract was calculated with the following formula:

$$A\beta_{1-42}\ aggregation\ inhibition\ (\%) = (1 - {}^{IF_i}\!/_{IF_c}) \times 100$$

Where IF_i and IF_c are the fluorescence intensities measured for A$\beta_{1–42}$ in the presence and absence of the inhibitors, respectively.

References:

Li, Q.; Tu, Y.; Zhu, C.; Luo, W.; Huang, W.; Liu, W.; Li, Y. Cholinesterase, *β*-amyloid aggregation inhibitory and antioxidant capacities of chinese medicinal plants. *Ind. Crop. Prod.* **2017**, *108,* 512−519.

Shi, Y. G.; Zhu, Y. J.; Shao, S. Y.; Zhang, R. R.; Wu, Y.; Zhu, C. M.; Liang, X. R.; Cai, W. Q. Alkyl ferulate esters as multi-functional food additives: Antibacterial activity and mode of action against *Escherichia coli* in vitro. *J. Agr. Food Chem.* **2018**, *66*(45), 12088−12101.

Shi, Y. G.; Wu, Y.; Lu, X. Y.; Ren Y. P.; Wang, Q.; Zhu, C. M.; Yu, D.; Wang, H. Lipase-catalyzed esterification of ferulic acid with lauryl alcohol in ionic liquids and antibacterial properties in vitro against three food-related bacteria. *Food Chem.* **2017**, *220*, 249–256.

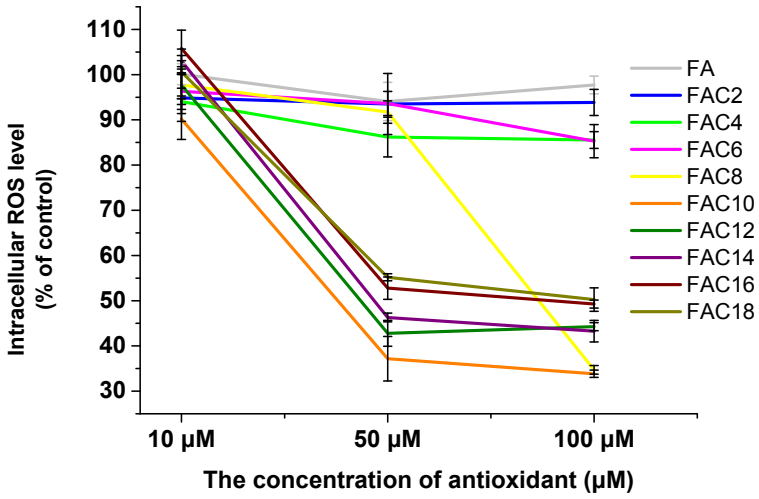

Figure 1S. Influence of a 24 h treatment with FA and its alkyl esters on ROS level in PC12 cells. Cells were pretreated with 10, 50 and 100 µM phenolic compound or 0.1% (v/v) ethanol (control cells) during 24 h. ROS level was assessed using DCF fluorescence using a microplate reader (λex: 485 nm/λem: 525 nm). Results are expressed as mean ± SD (n=3).

FA

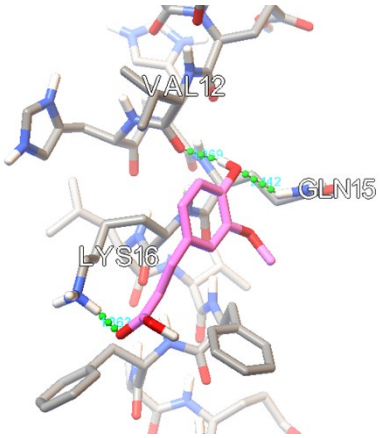

FAC2

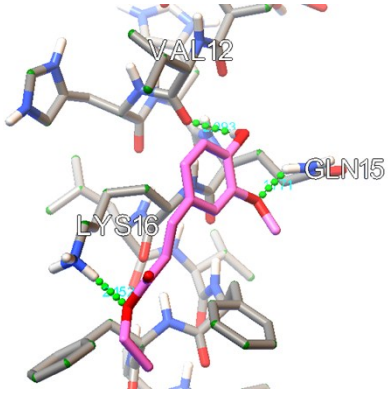

FAC4

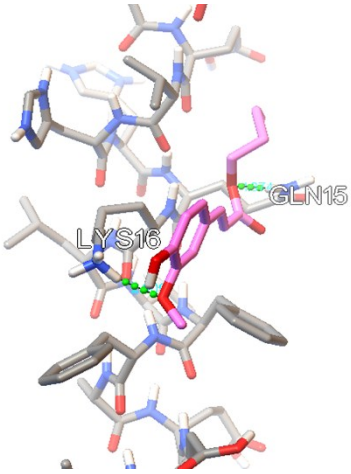

FAC6

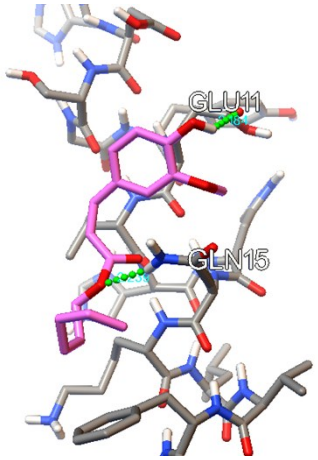

FAC8

FAC10

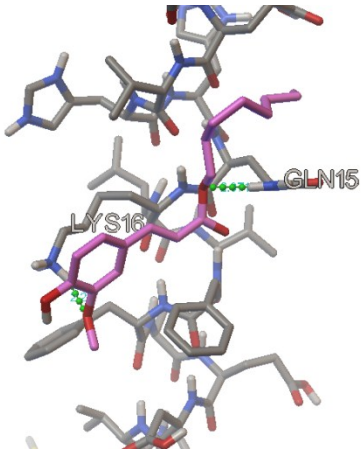

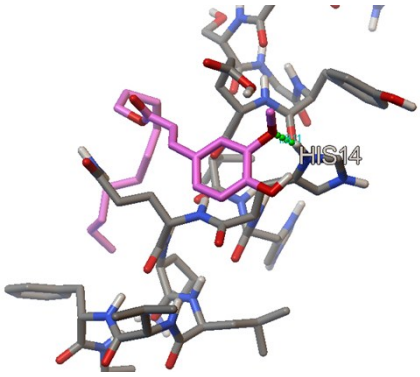

FAC12 **FAC14**

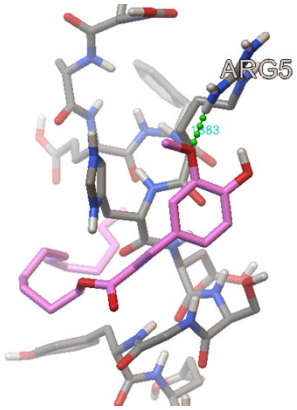

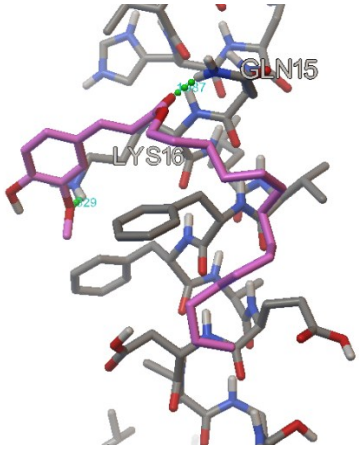

Figure 2S. Docking model between A$\beta_{1\text{-}42}$ monomer and FAEs calculated by AutoDock.

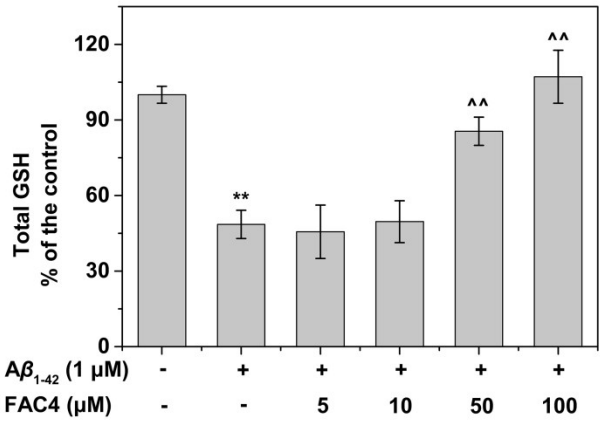

Fig. 3S. Effect of FAC4 upon GSH content in PC12 cells. PC12 cells were seeded in 6-well plates (5×10^5 cells per well) for 1 day and subsequently treated with indicated concentrations of A$\beta_{1\text{-}42}$ and FAC4 for another 24 h. Then, the cells were collected and detected as described in the Methods. All data represent the means ± SD of three independent experiments. *, $P < 0.05$, **, $P < 0.01$ vs the control group; ^, $P < 0.05$, and ^^, $P < 0.01$ the A$\beta_{1\text{-}42}$-treated group.

[Table 1S. Structural properties and binding interactions of FA and FAEs into the A$\beta_{1\text{-}42}$ active site calculated by the docking study.]

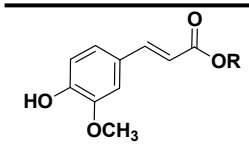		R	miLog*P*[a]	*c*Log*P*[b]	ΔG_b（Kcal/mol）	K_i(μM)	Atom of the ligand	Amino acid
Ferulic acid	**FA**	H	1.25	1.4212	-4.5	503.96	4-OH	VAL12
							4-OH	GLN15
							C=O	LYS16
	FAC2	C_2H_5	2.24	2.1762	-4.23	791.78	4-OH	VAL12
							$3\text{-}OCH_3$	GLN15
							C-O-C	LYS16
Ferulic alkyl esters	**FAC4**	C_4H_9	3.30	3.2342	-3.95	1.28 mM	C-O-C	GLN15
							$3\text{-}OCH_3$	LYS16
	FAC6	C_6H1_3	4.31	4.2922	-3.65	2.11 mM	4-OH	GLU11
							C-O-C	GLN15
	FAC8	C_8H_{17}	5.32	5.3502	-3.86	1.49 mM	C-O-C	GLN15
							$3\text{-}OCH_3$	LYS16

	FAC10	$C_{10}H_{21}$	6.33	6.4082	-3.41	3.15 mM	3-OCH_3	HIS14
	FAC12	$C_{12}H_{25}$	7.34	7.4662	-3.44	3.01 mM	3-OCH_3	ARG5
	FAC 14	$C_{14}H_{27}$	8.30	8.5242	-3.16	4.79 mM	C=O 3-OCH_3	GLN15 LYS16
	FAC 16	$C_{16}H_{31}$	8.86	9.5822	-2.34	19.11 mM		
	FAC 18	$C_{18}H_{35}$	9.22	10.6402	-2.23	23.13 mM		

[a]The data was determined with Molinspiration calculation software. [b] Theoretical estimated using ChemBioDraw Ultra 13.0 program.

NMR (^{13}C NMR), MS, and HPLC data of FAEs synthesized through biotransformation in this work have been provided here.

FAC2

^{13}C NMR (600 MHz, $CDCl_3$) δ 167.28 (9-C=O), 147.89 (3-C-O-CH_3), 146.74 (4-C-OH), 144.66 (7-CH=CH), 127.05 (1-C), 123.02 (6-CH), 115.66 (8-C-C=O), 114.70 (5-CH), 109.29 (2-CH), 60.37 (1'-O-CH_2), 55.9 (10-CH_3-O-Ar), 14.36 (4'-CH_3).

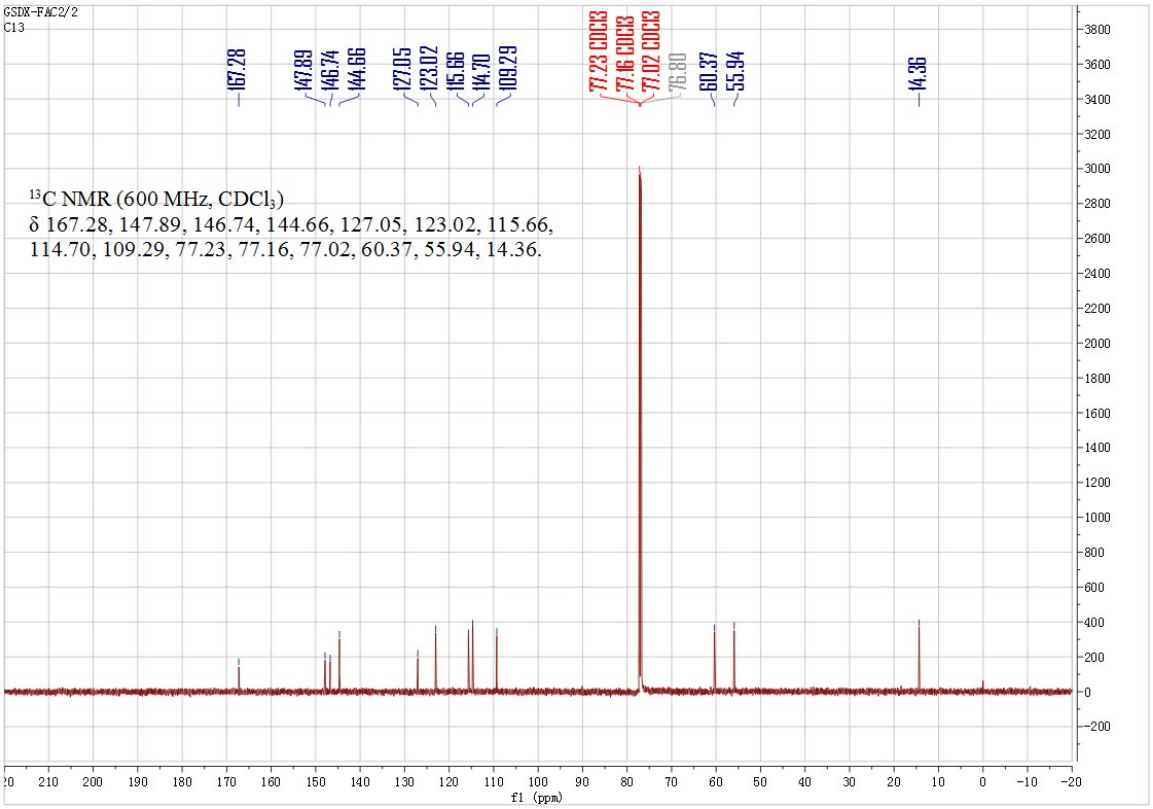

MS^1 (223.08)

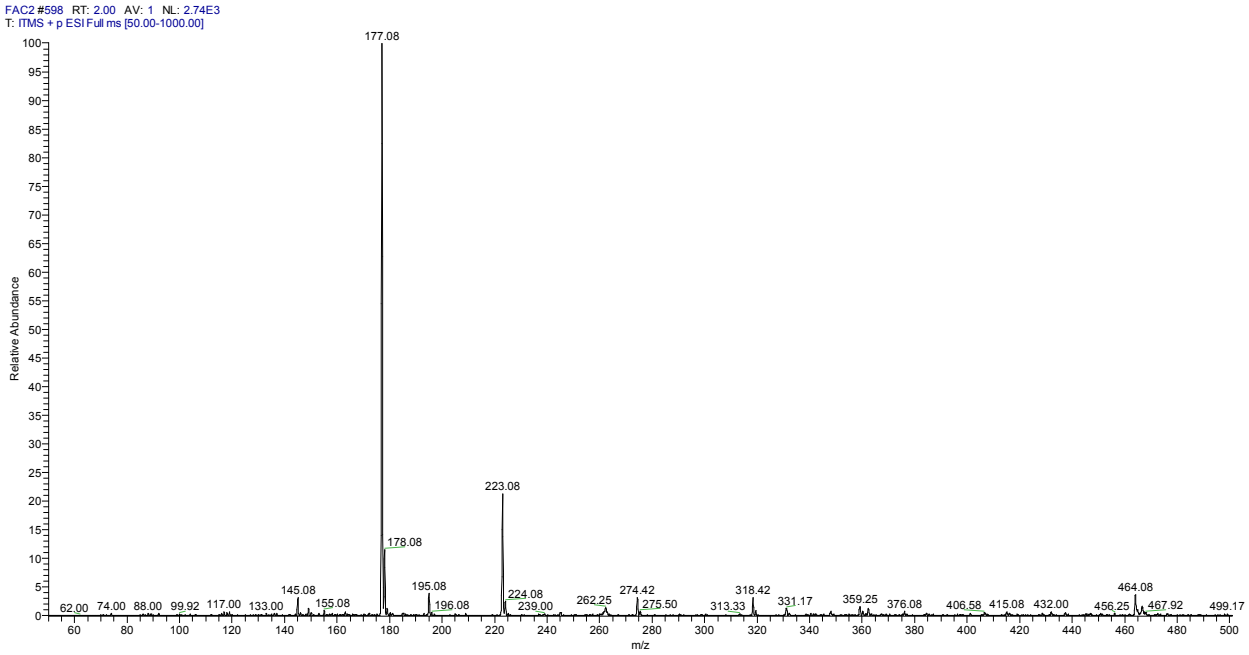

MS^2 (177.08)

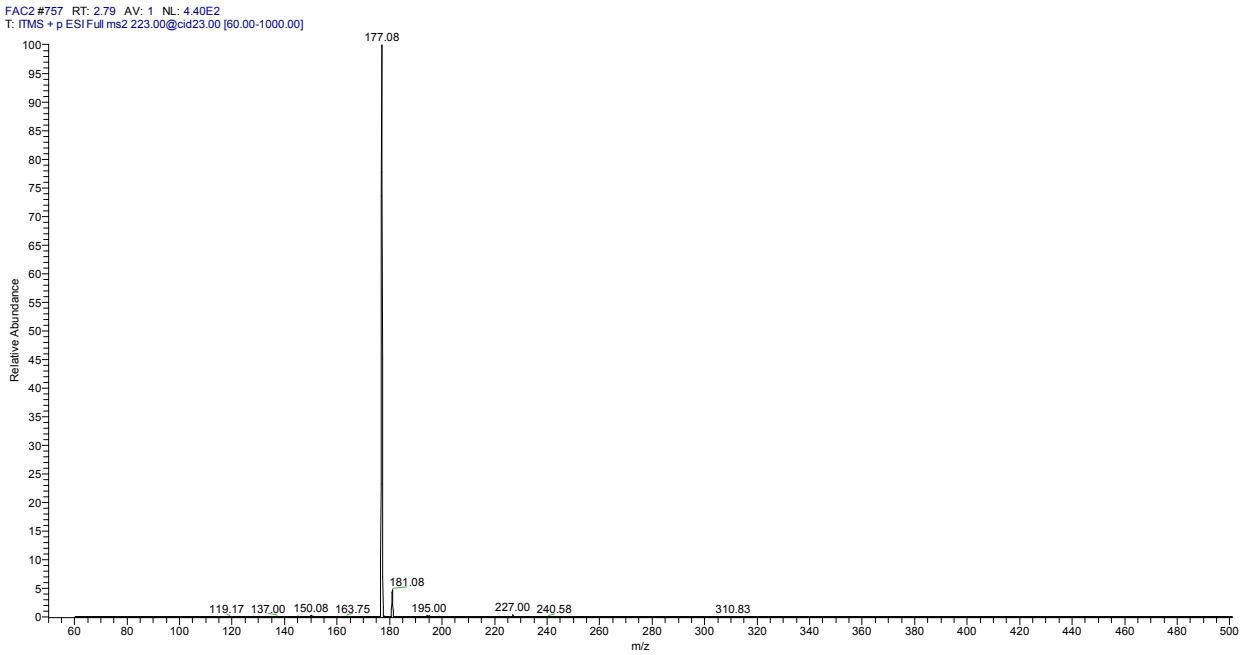

FAC4

^{13}C NMR (600 MHz, $CDCl_3$) δ 167.4 (9-C=O), 147.9 (3-C-O-CH_3), 146.7 (4-C-OH), 144.6 (7-CH=CH), 127.0 (1-C), 123.0 (6-CH), 115.6 (8-C-C=O), 114.7 (5-CH), 109.3 (2-CH), 64.3 (1'-O-CH_2), 55.9 (10-CH_3-O-Ar), 30.8 (2'-CH_2), 19.2 (3'-CH_2), 13.7 (4'-CH_3).

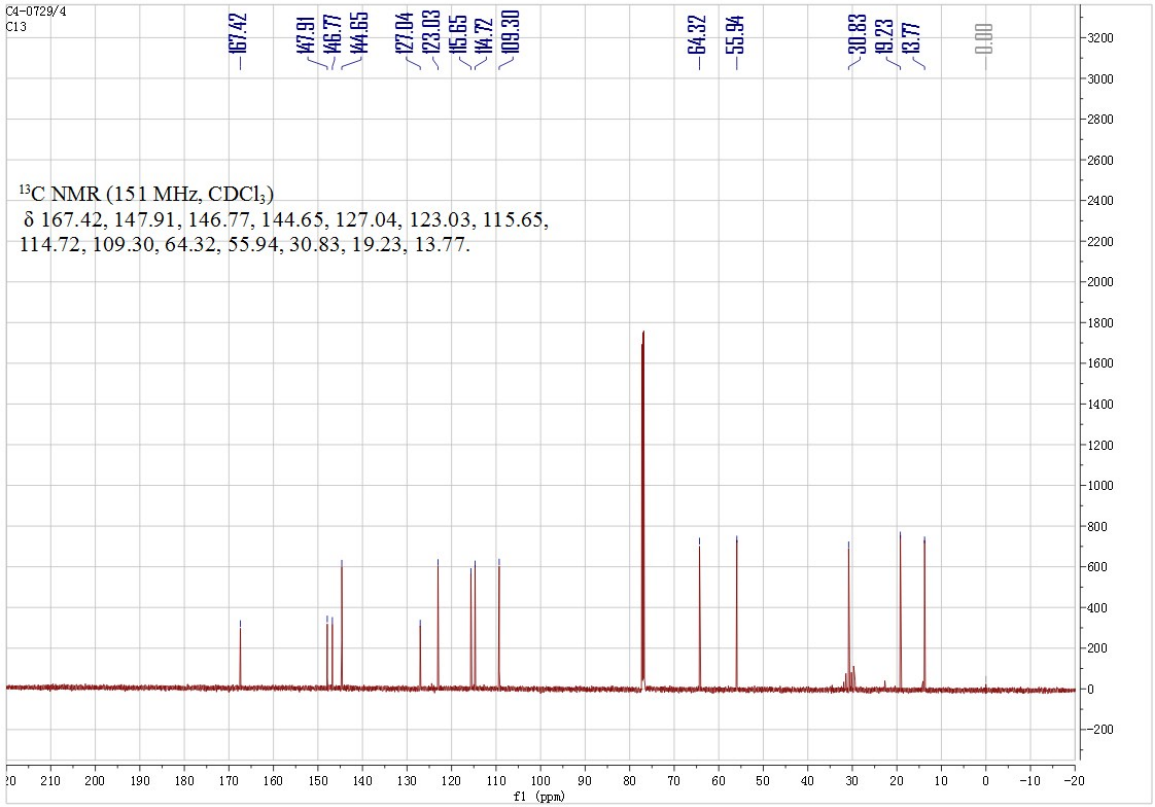

MS[1] (251.00)

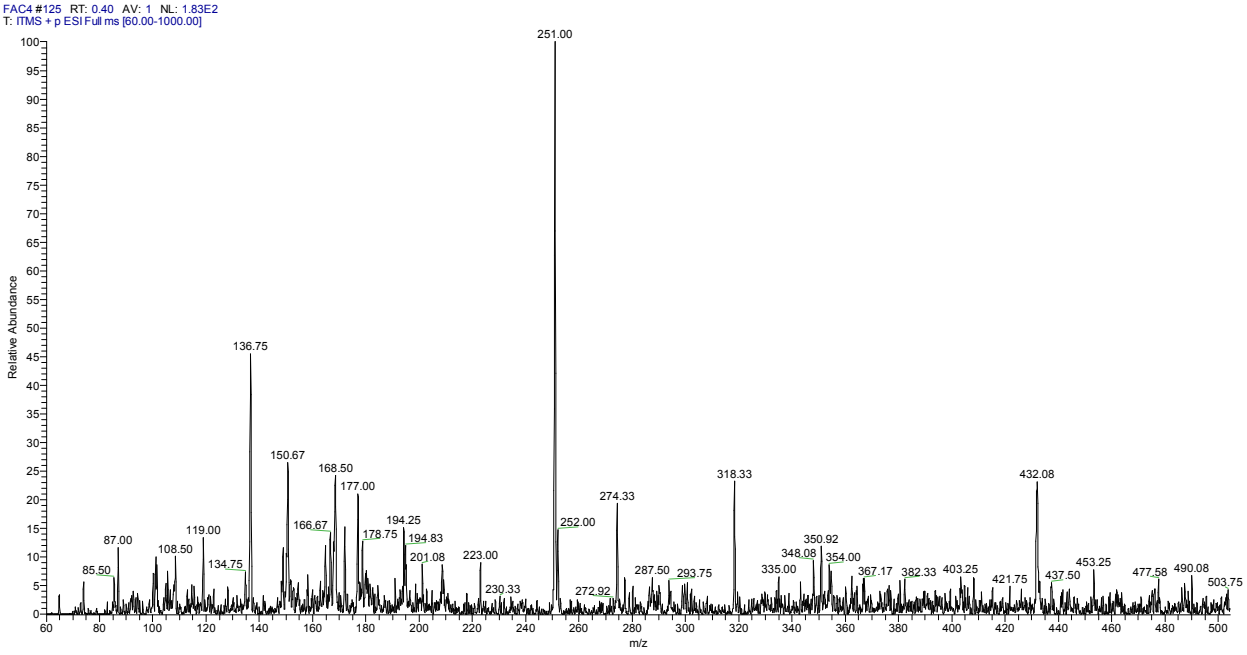

MS[2] (177.08)

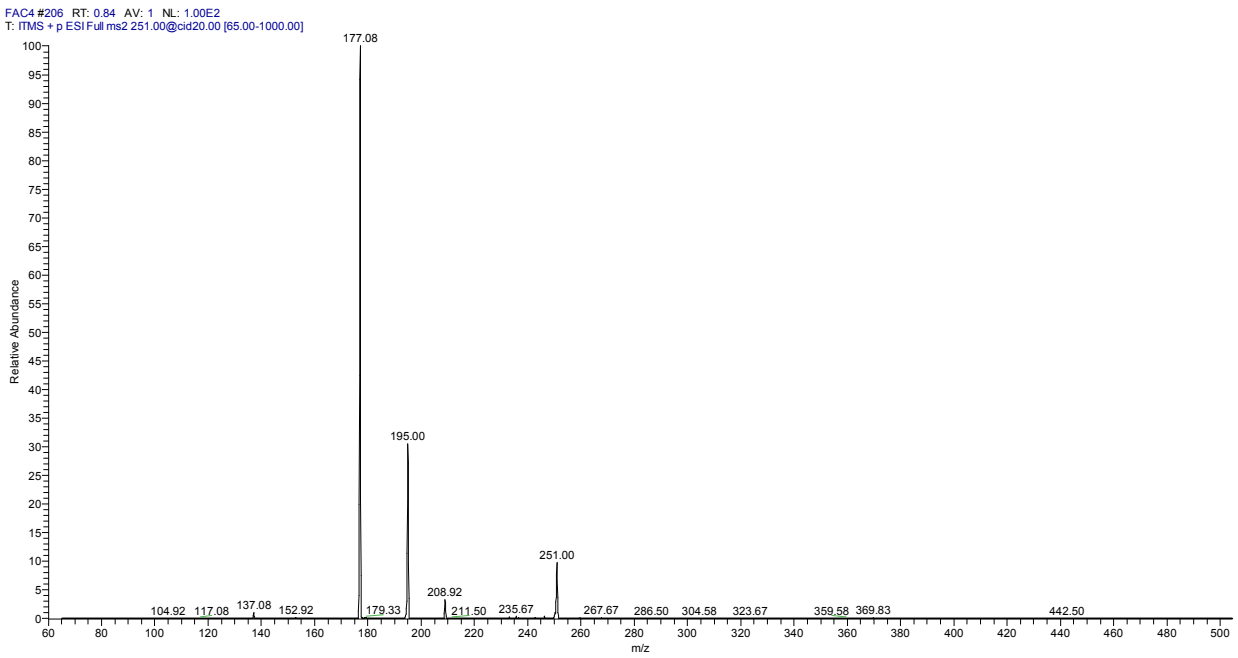

FAC6

^{13}C NMR (600 MHz, $CDCl_3$) δ 167.63 (9-C=O), 148.19 (3-C-O-CH_3), 147.03 (4-C-OH), 144.87 (7-CH=CH), 126.92 (1-C), 123.01 (6-CH), 115.42 (8-C-C=O), 114.97 (5-CH), 109.58 (2-CH), 64.6 9(1'-O-CH_2), 55.89 (10-CH_3-O-Ar), 31.51 (2'-CH_2), 28.75 (3'-CH_2), 25.69 (4'-CH_2), 22.59 (5'-CH_2), 14.04 (6'-CH_3)

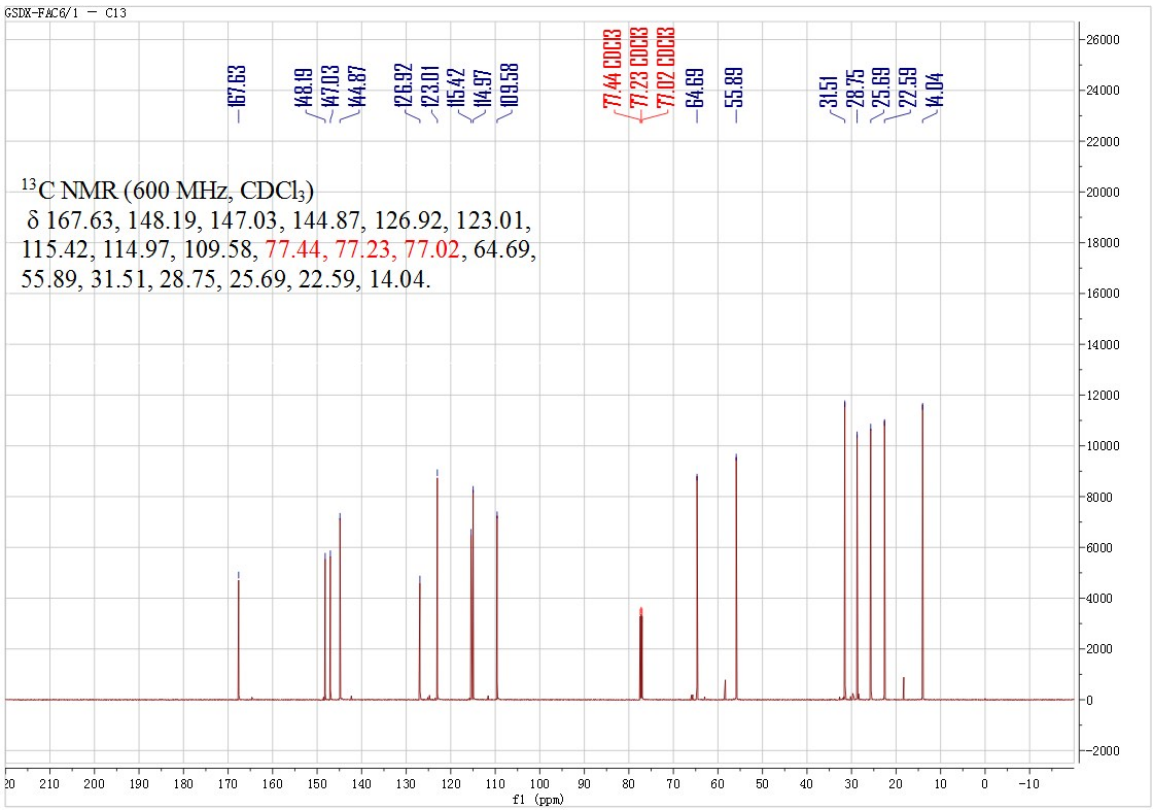

MS[1] (279.08)

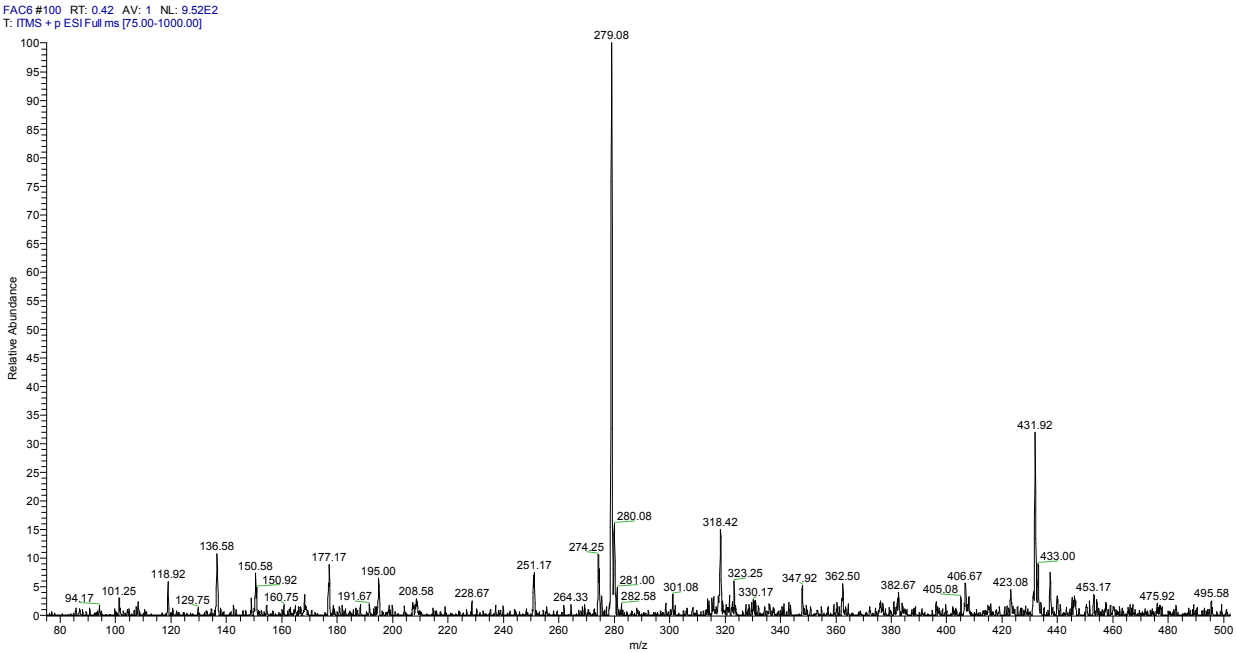

MS[2] (177.00)

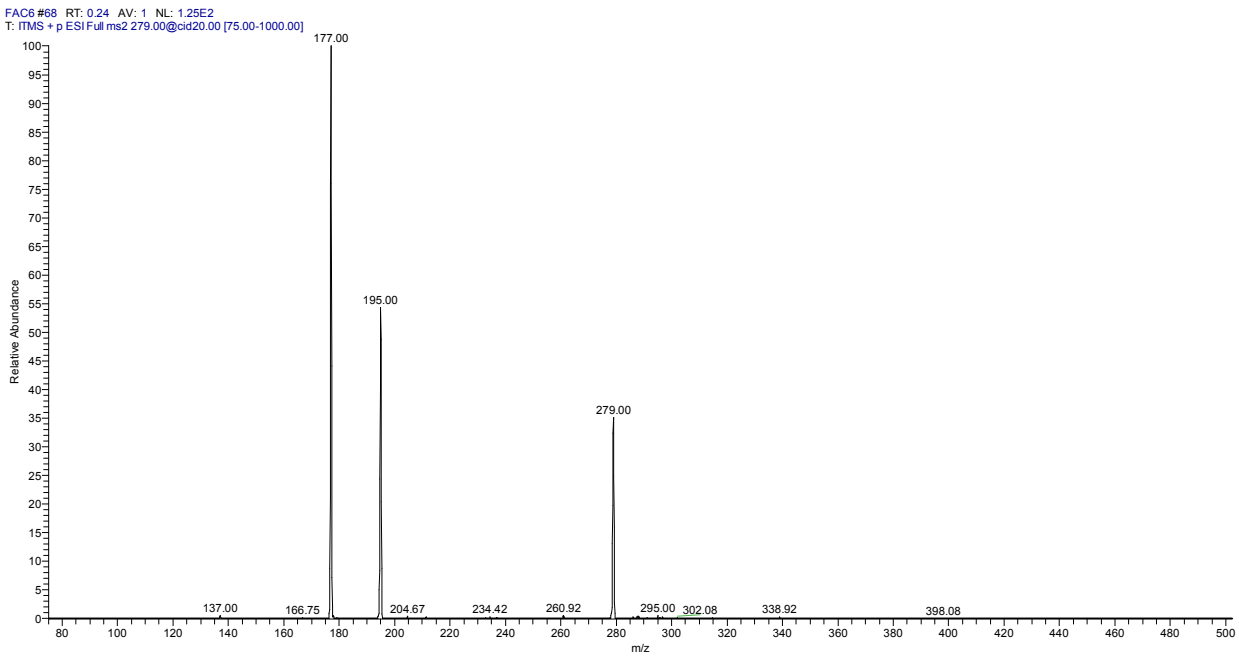

FAC8

^{13}C NMR (600 MHz, $CDCl_3$) δ 167.66 (9-C=O), 148.28 (3-C-O-CH_3), 147.10 (4-C-OH), 144.92 (7-CH=CH), 126.90 (1-C), 123.00 (6-CH), 115.36 (8-C-C=O), 115.04 (5-CH), 109.66 (2-CH), 64.71 (1'-O-CH_2), 55.85 (10-CH_3-O-Ar), 31.85 (2'-CH_2), 29.32 (3'-CH_2), 29.26 (4'-CH_2), 28.81 (5'-CH_2), 26.05 (6'-CH_2), 22.70 (7'-CH_2), 14.12(8'-CH_3).

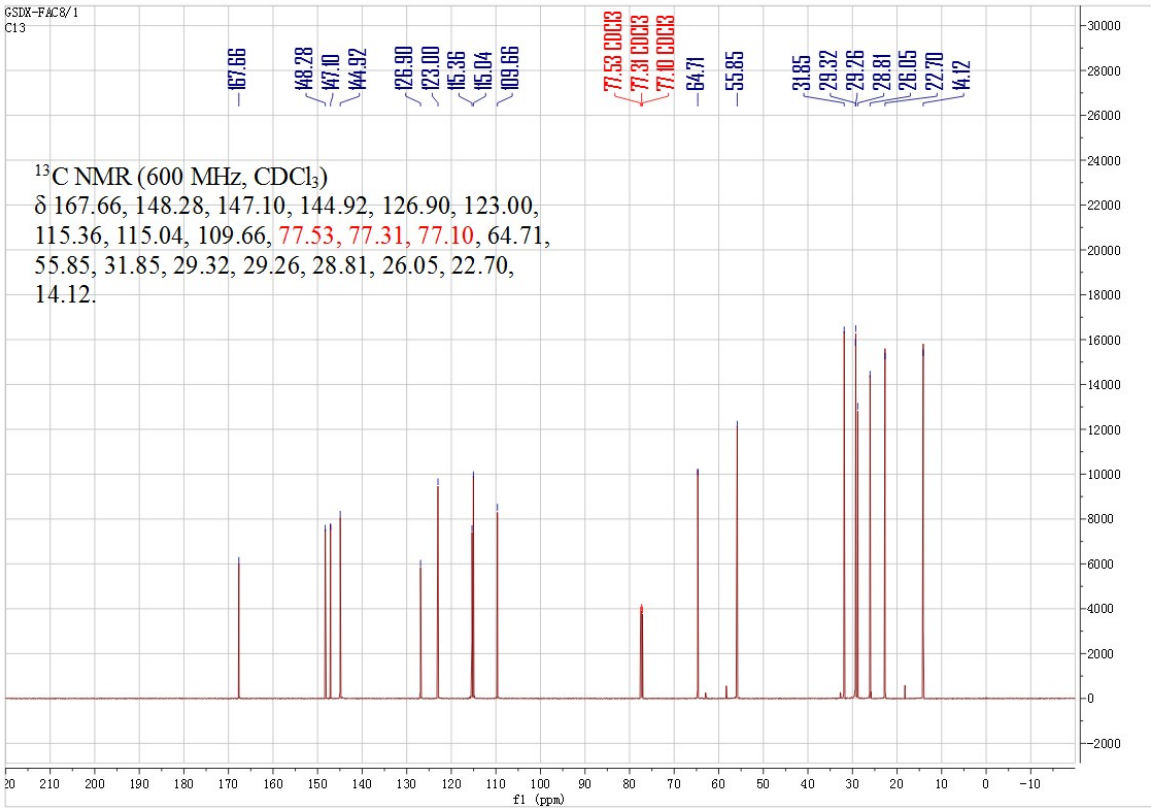

MS[1] (307.40)

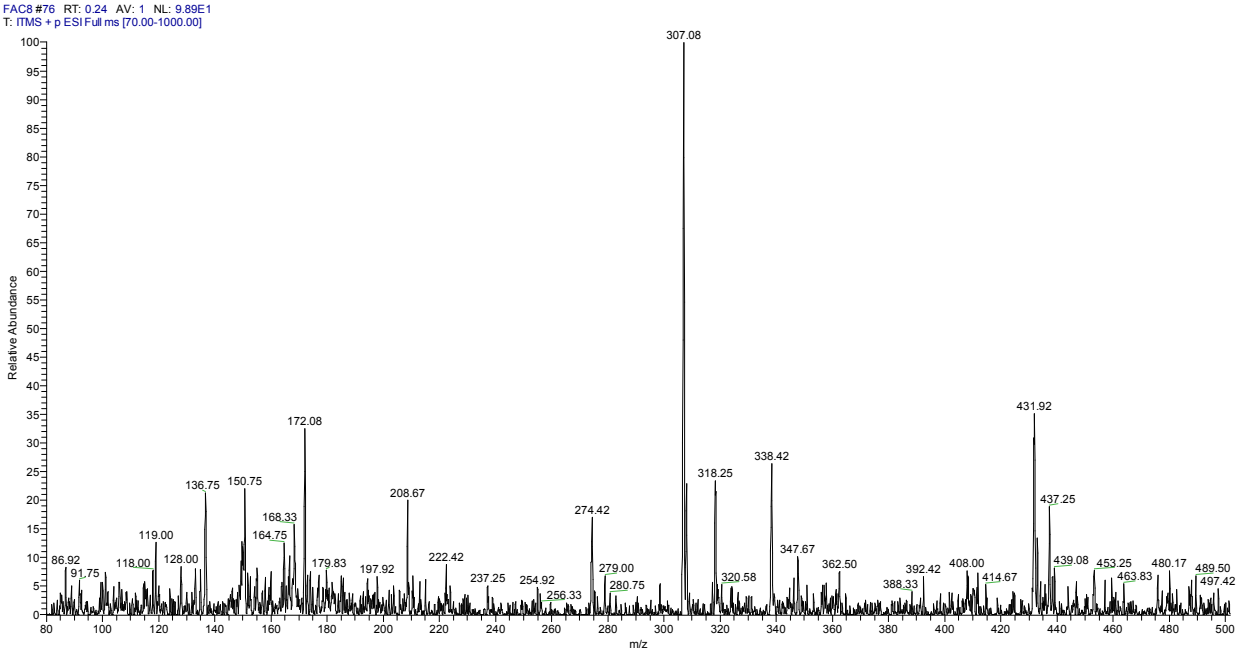

MS[2] (177.00)

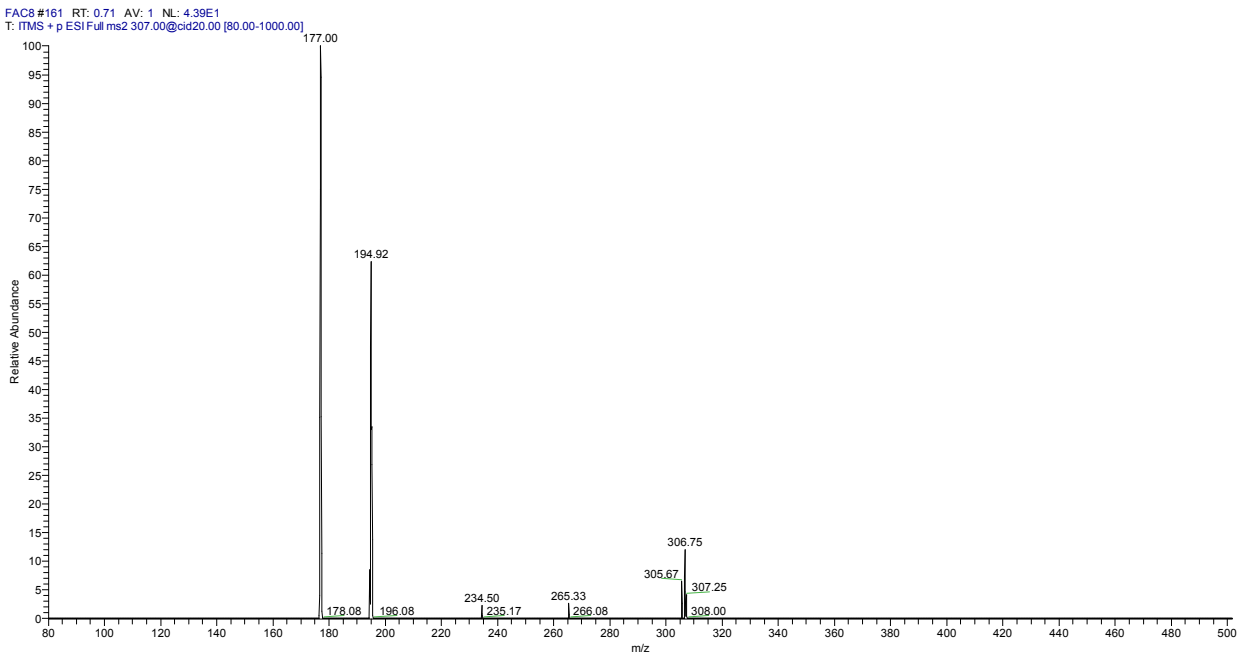

FAC10

^{13}C NMR (600 MHz, $CDCl_3$): δ 167.44 (9-C=O), 147.95 (3-C-O-CH_3), 146.82 (4-C-OH), 144.67 (7-CH=CH), 127.03 (1-C), 123.04 (6-CH), 115.65 (8-C-C=O), 114.76 (5-CH), 109.36(2-CH), 64.65 (1'-O-CH_2), 55.95 (10-CH_3-O-Ar), 31.90 (2'-CH_2), 29.56 (3'-CH_2), 29.56 (4'-CH_2), 29.32 (5'-CH_2), 29.31 (6'-CH_2), 28.78 (7'-CH_2), 26.01 (8'-CH_2), 22.69 (9'-CH_2), 14.12 (10'-CH_2).

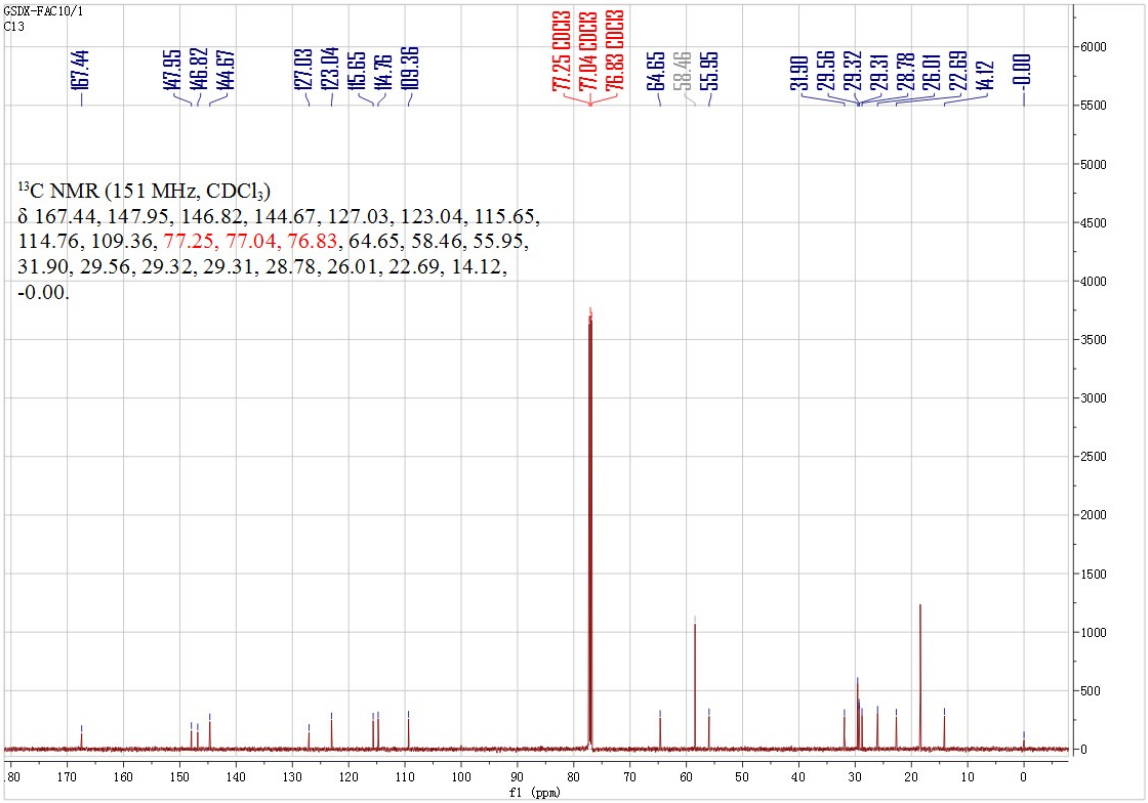

MS[1] (335.45)

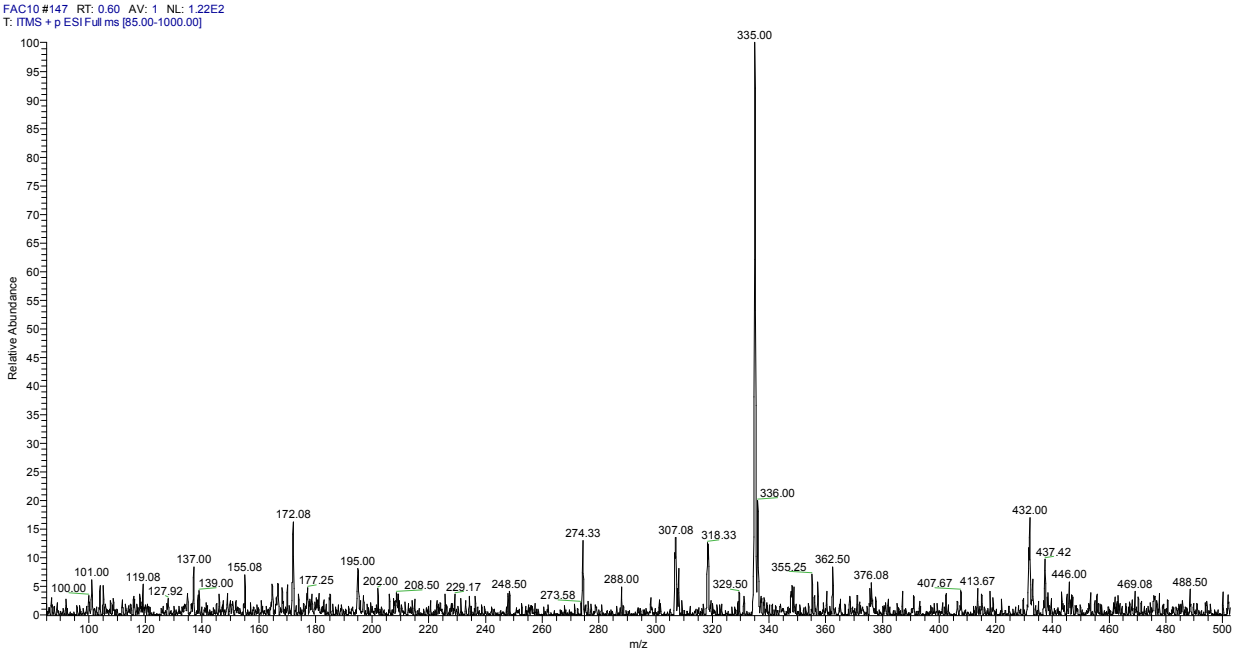

MS[2] (177.00)

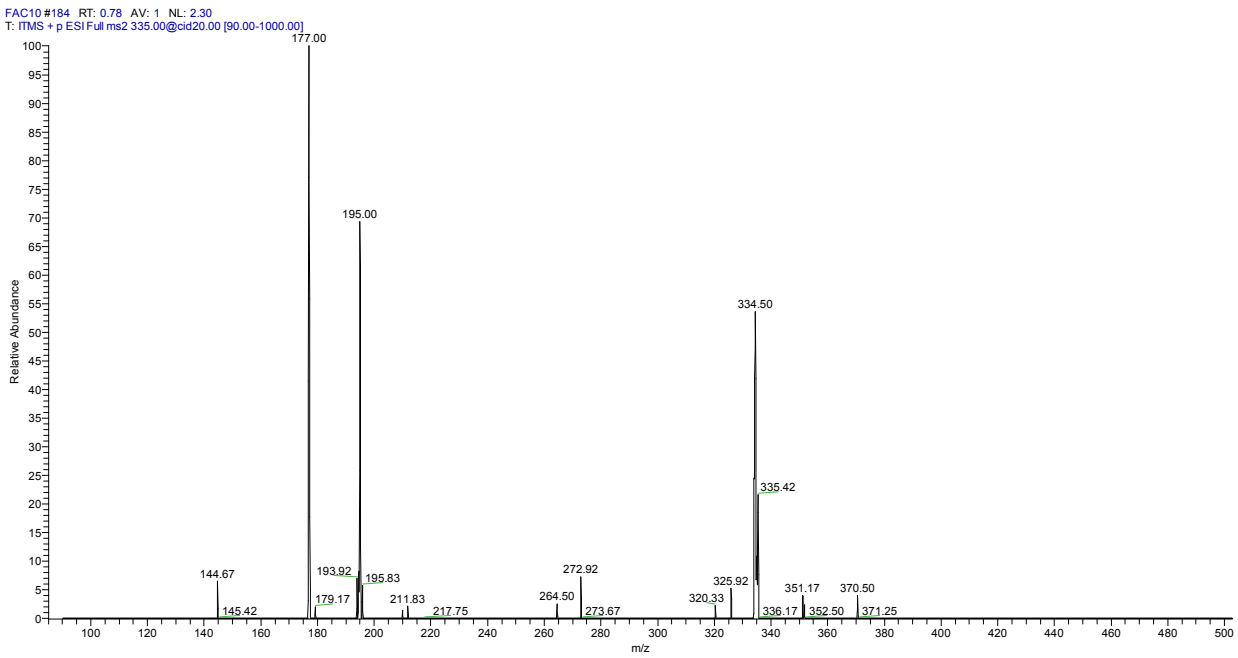

FAC12

^{13}C NMR (600 MHz, $CDCl_3$): 167.49 (9-C=O), 148.02 (3-C-O-CH_3), 146.88 (4-C-OH), 144.71 (7-CH=CH), 127.01 (1-C), 123.05 (6-CH), 115.6 (8-C-C=O), 114.82 (5-CH), 109.43 (2-CH), 64.6 6(1'-O-CH_2), 55.95 (10-CH_3-O-Ar), 31.93 (2'-CH_2), 29.67 (3'-CH_2), 29.65 (4'-CH_2), 29.61 (5'-CH_2), 29.56 (6'-CH_2), 29.36 (7'-CH_2), 29.32 (8'-CH_2), 28.79 (9'-CH_2), 26.02 (10'-CH_2), 22.70 (11'-CH_2), 14.12 (12'-CH_3).

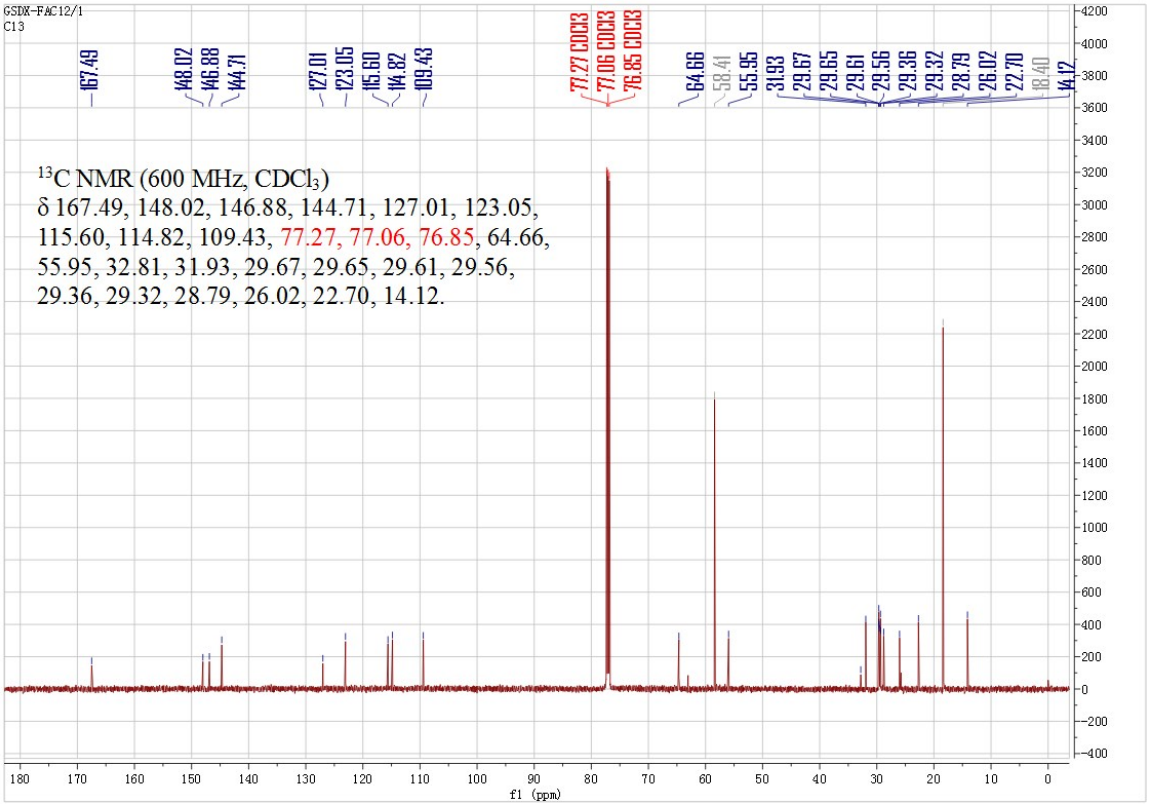

MS[1] (363.08)

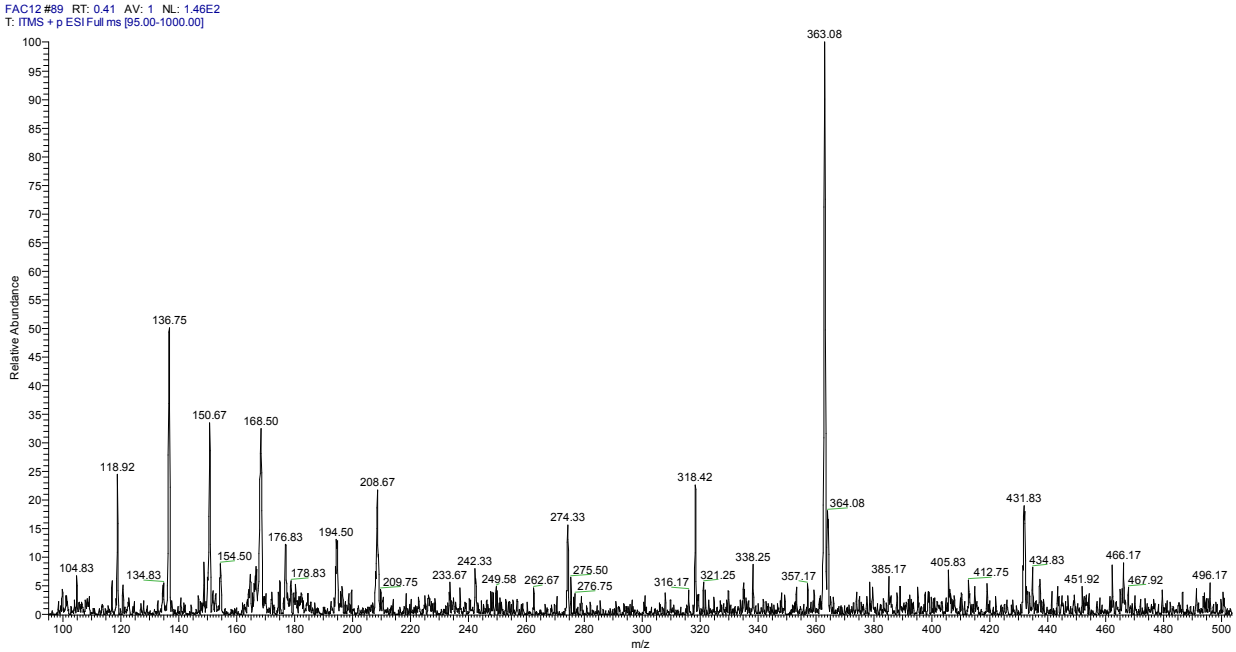

MS[2] (177.00)

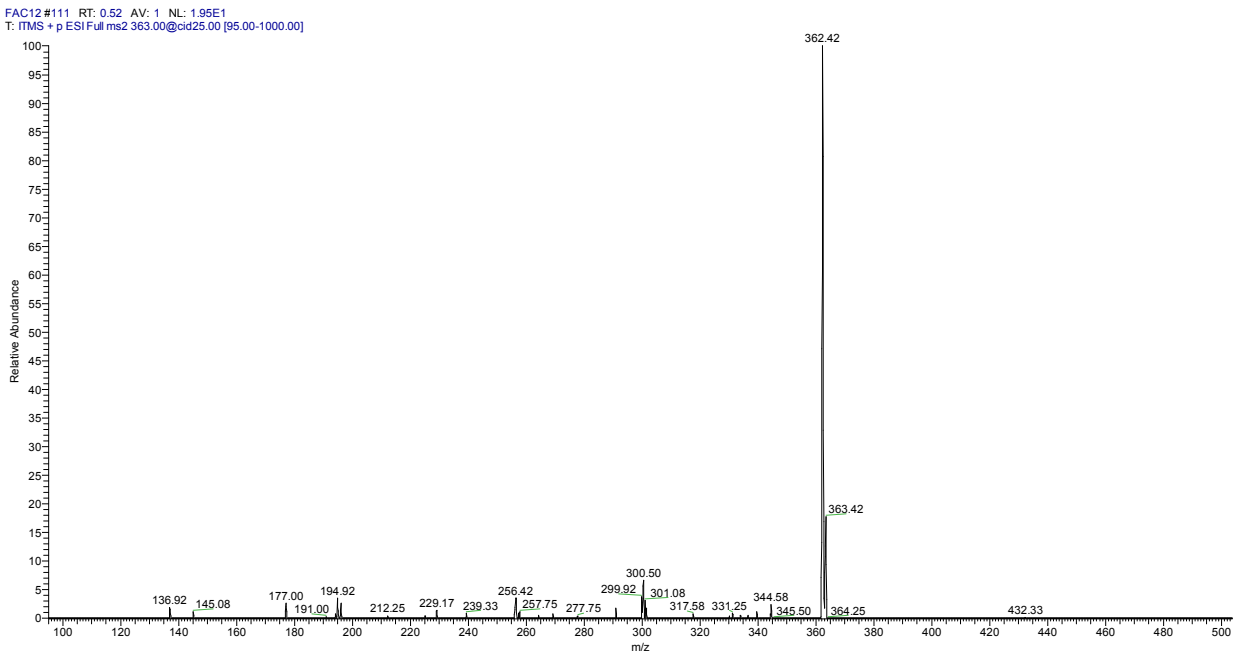

FAC14

^{13}C NMR (600 MHz, $CDCl_3$): 167.38 (9-C=O), 147.88 (3-C-O-CH_3), 146.74 (4-C-OH), 144.61 (7-CH=CH), 127.06 (1-C), 123.04 (6-CH), 115.69 (8-C-C=O), 114.69 (5-CH), 109.28 (2-CH), 64.62 (1'-O-CH_2), 55.94 (10-CH_3-O-Ar), 31.93 (2'-CH_2), 29.70 (3'-CH_2), 29.68 (4'-CH_2), 29.66 (5'-CH_2), 29.60 (6'-CH_2), 29.55, 29.31, 28.78, 26.01, 22.70 (7', 8' ,9' , 10', 11', 12', 13'-CH_2), 14.12 (14'-CH_3).

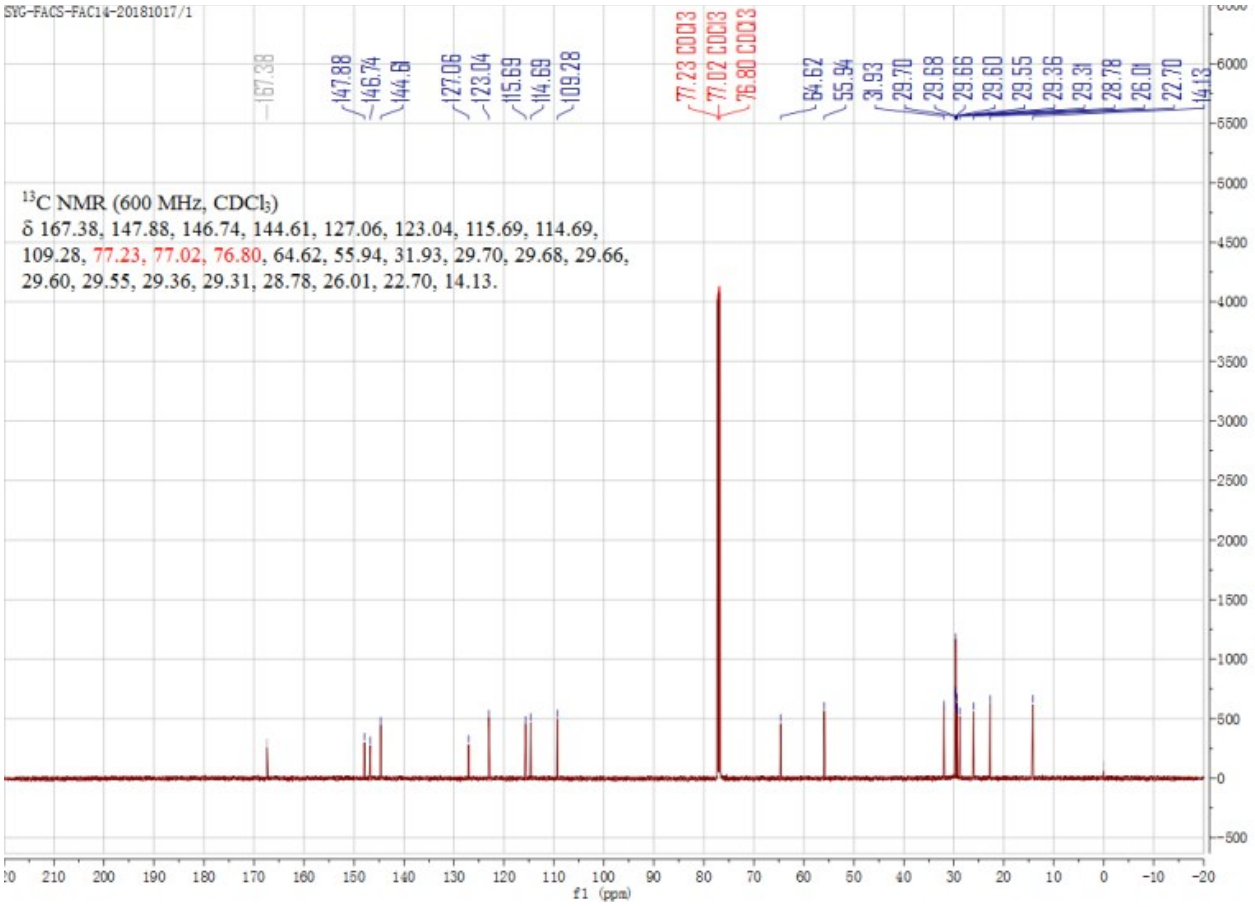
SYG-FACS-FAC14-20181017/1
167.38
147.88
146.74
144.61
127.06
123.04
115.69
114.69
109.28
77.23 CDCl3
77.02 CDCl3
76.80 CDCl3
64.62
55.94
31.93
29.70
29.68
29.66
29.60
29.55
29.36
29.31
28.78
26.01
22.70
14.13
13C NMR (600 MHz, CDCl3)
δ 167.38, 147.88, 146.74, 144.61, 127.06, 123.04, 115.69, 114.69,
109.28, 77.23, 77.02, 76.80, 64.62, 55.94, 31.93, 29.70, 29.68, 29.66,
29.60, 29.55, 29.36, 29.31, 28.78, 26.01, 22.70, 14.13.
f1 (ppm)

MS^1(391.42)

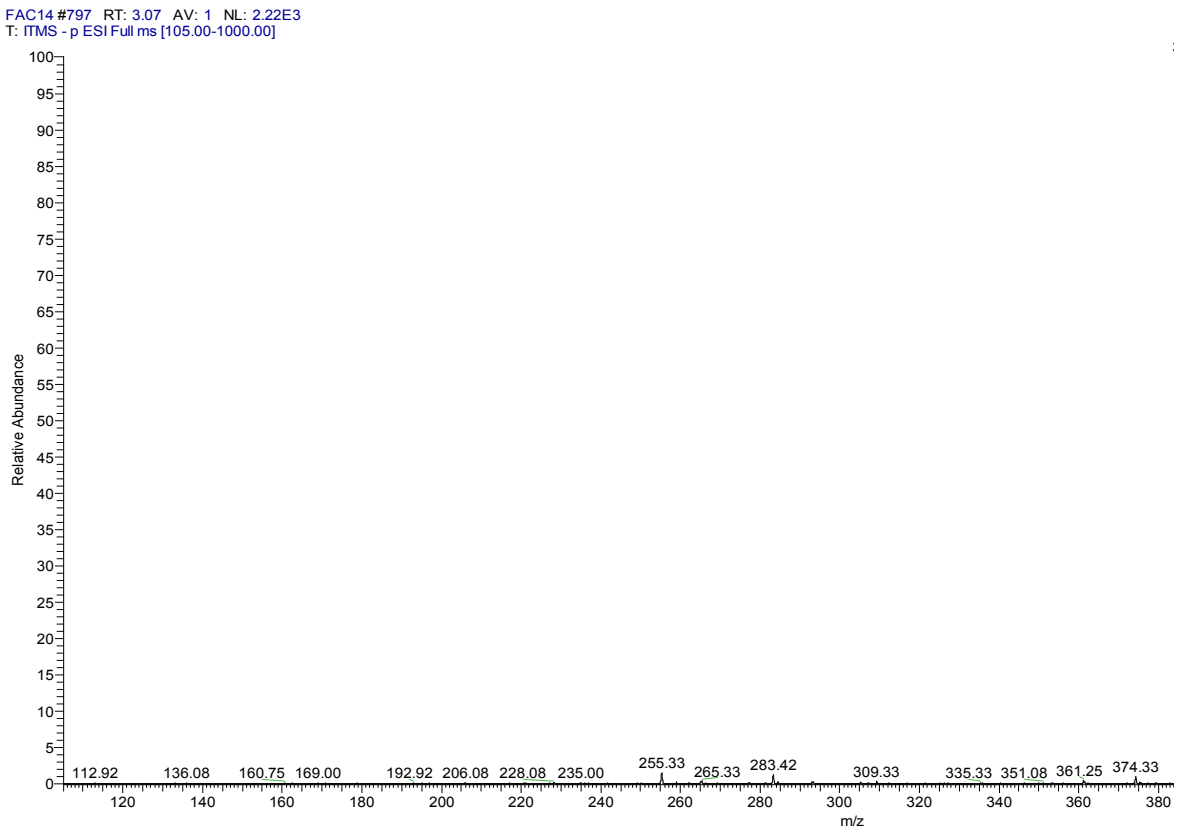
FAC14 #797 RT: 3.07 AV: 1 NL: 2.22E3
T: ITMS - p ESI Full ms [105.00-1000.00]
Relative Abundance
m/z
112.92
136.08
160.75
169.00
192.92
206.08
228.08
235.00
255.33
265.33
283.42
309.33
335.33
351.08
361.25
374.33

MS^2

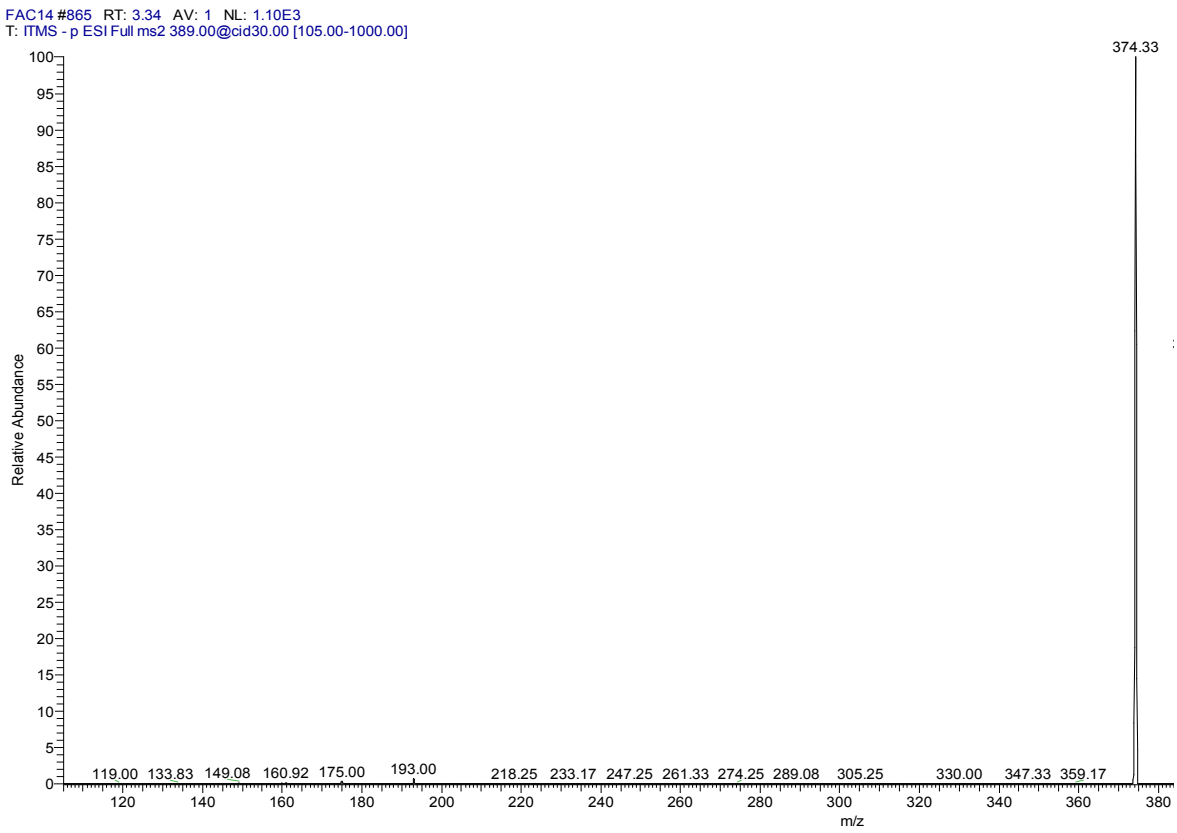

FAC16

^{13}C NMR (600 MHz, $CDCl_3$): 167.38 (9-C=O), 147.88 (3-C-O-CH_3), 146.74 (4-C-OH), 144.61 (7-CH=CH), 127.06 (1-C), 123.04 (6-CH), 115.69 (8-C-C=O), 114.69 (5-CH), 109.28 (2-CH), 64.62 (1'-O-CH_2), 55.94 (10-CH_3-O-Ar), 31.93 (2'-CH_2), 29.70 (3'-CH_2), 29.66 (4'-CH_2), 29.61 (5'-CH_2), 29.56 (6'-CH_2), 29.37, 29.32, 28.79, 26.01, 22.70 (7', 8', 9', 10', 11', 12', 13', 14', 15'-CH_2), 14.12 (16'-CH_3).

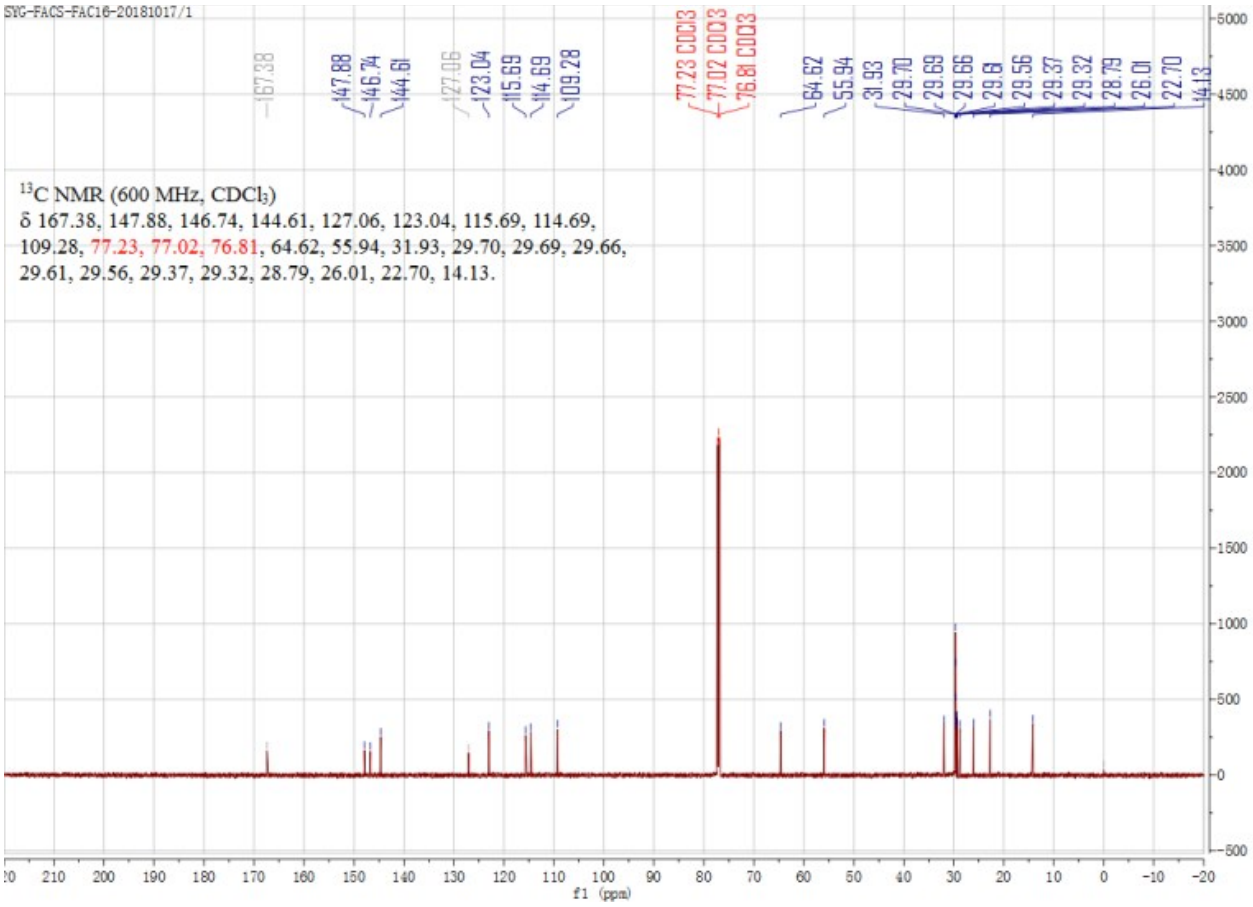
SYG-FACS-FAC16-20181017/1
167.38
147.88
146.74
144.61
127.06
123.04
115.69
114.69
109.28
77.23 CDCl3
77.02 CDCl3
76.81 CDCl3
64.62
55.94
31.93
29.70
29.69
29.66
29.61
29.56
29.37
29.32
28.79
26.01
22.70
14.13
13C NMR (600 MHz, CDCl3)
δ 167.38, 147.88, 146.74, 144.61, 127.06, 123.04, 115.69, 114.69,
109.28, 77.23, 77.02, 76.81, 64.62, 55.94, 31.93, 29.70, 29.69, 29.66,
29.61, 29.56, 29.37, 29.32, 28.79, 26.01, 22.70, 14.13.
f1 (ppm)

MS^1(419.33)

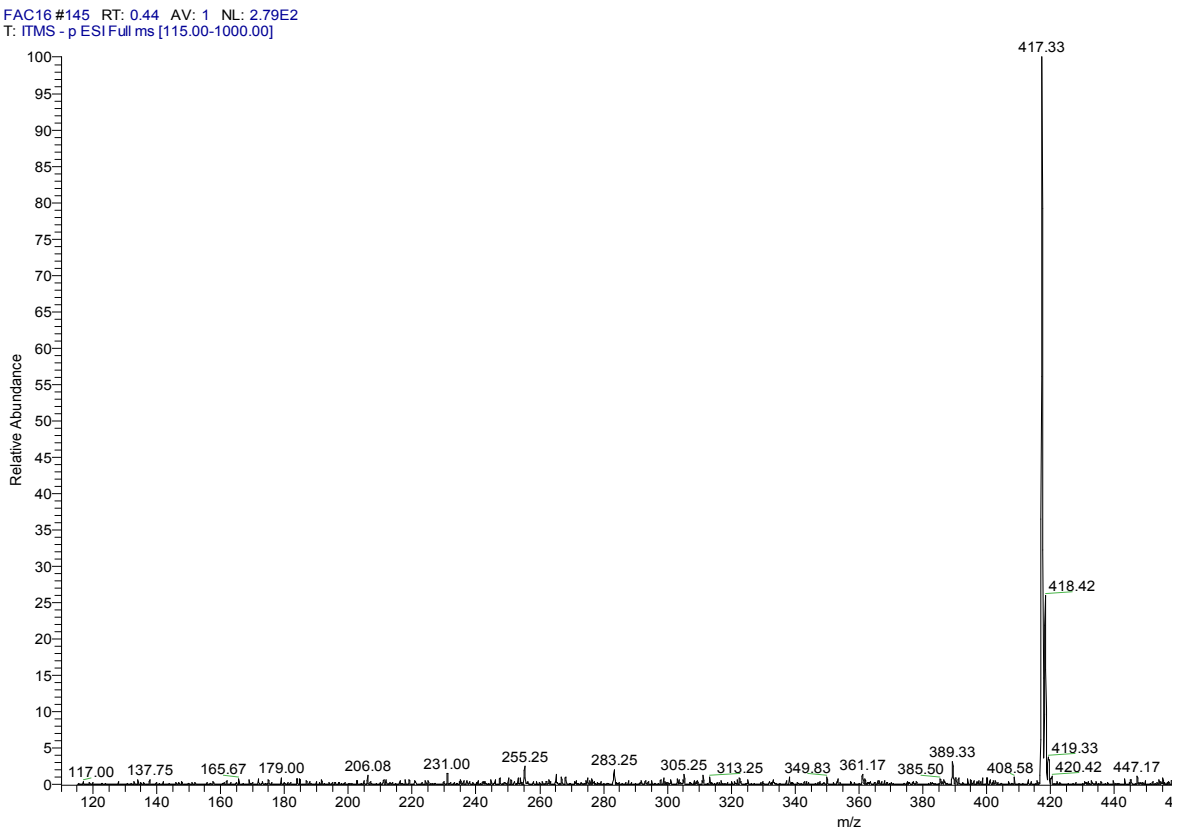
FAC16 #145 RT: 0.44 AV: 1 NL: 2.79E2
T: ITMS - p ESI Full ms [115.00-1000.00]
Relative Abundance
m/z
417.33
418.42
419.33
420.42
389.33
117.00
137.75
165.67
179.00
206.08
231.00
255.25
283.25
305.25
313.25
349.83
361.17
385.50
408.58
447.17

MS^2

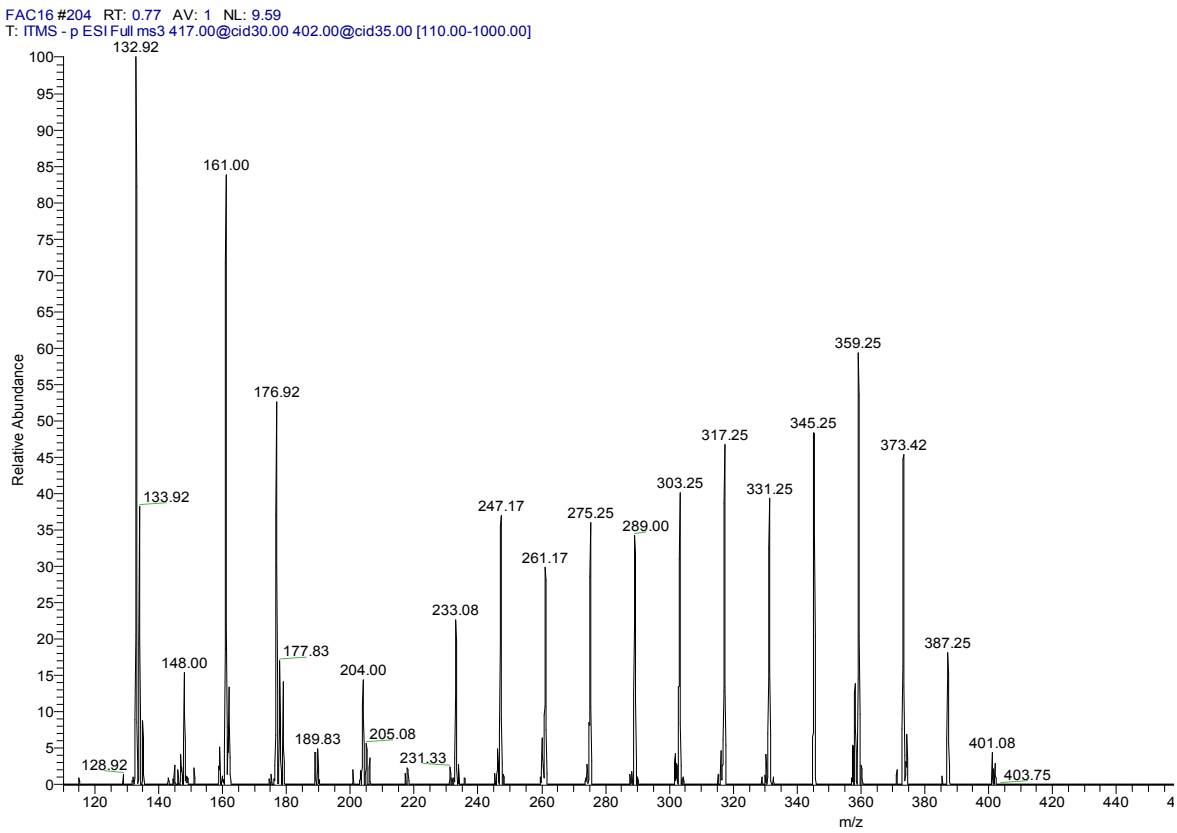

FAC18

^{13}C NMR (600 MHz, $CDCl_3$): 167.37 (9-C=O), 147.87 (3-C-O-CH_3), 146.73 (4-C-OH), 144.60 (7-CH=CH), 127.07 (1-C), 123.04 (6-CH), 115.70 (8-C-C=O), 114.68 (5-CH), 109.27 (2-CH), 64.62 (1'-O-CH_2), 55.95 (10-CH_3-O-Ar), 31.93 (2'-CH_2), 29.70 (3'-CH_2), 29.69 (4'-CH_2), 29.66 (5'-CH_2), 29.61, 28.56, 29.37, 29.32, 28.78, 26.01, 22.70 (6', 7', 8' ,9' , 10', 11', 12', 13', 14', 15', 16', 17'-CH_2), 14.12 (18'-CH_3).

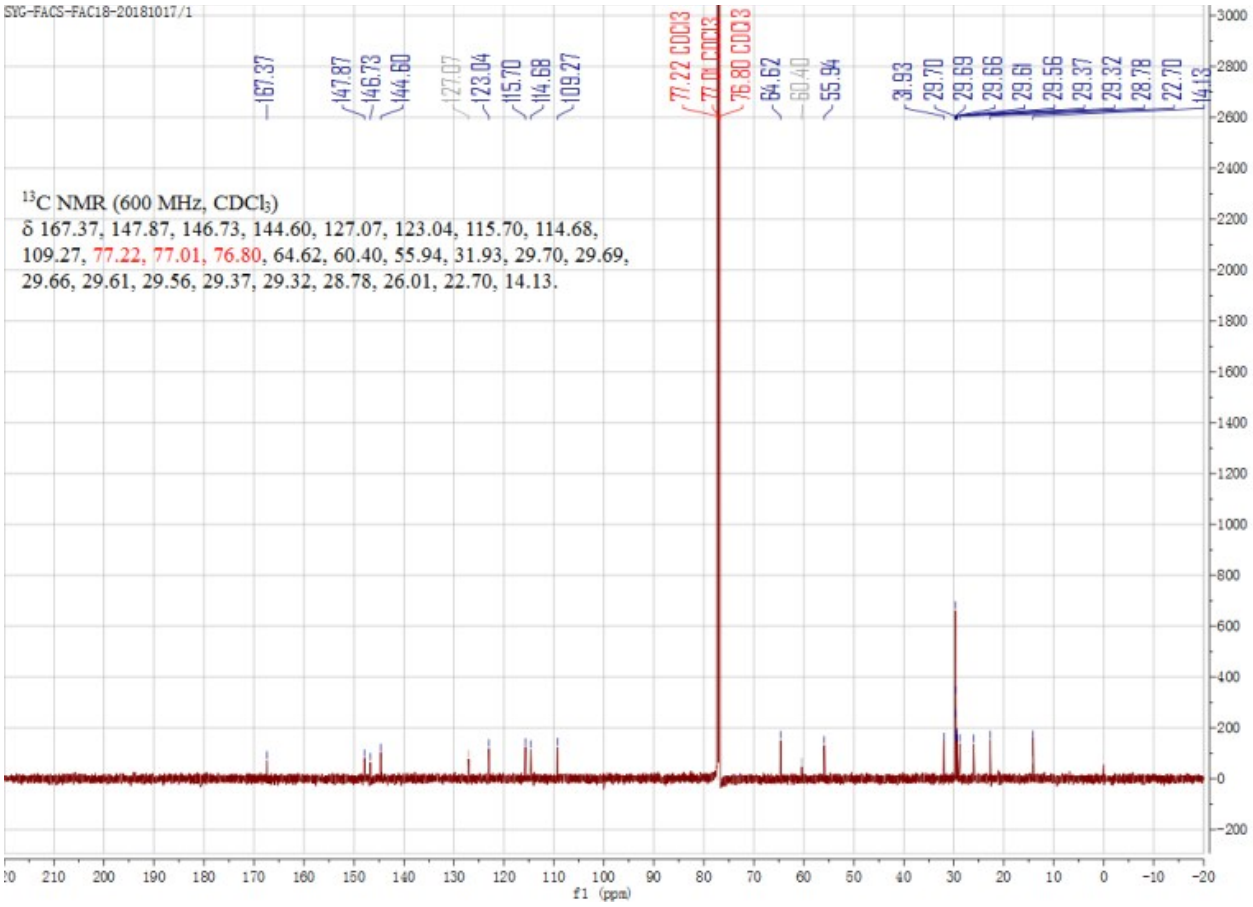
SYG-FACS-FAC18-20181017/1
167.37
147.87
146.73
144.60
127.07
123.04
115.70
114.68
109.27
77.22 CDCl3
77.01 CDCl3
76.80 CDCl3
64.62
60.40
55.94
31.93
29.70
29.69
29.66
29.61
29.56
29.37
29.32
28.78
22.70
14.13
13C NMR (600 MHz, CDCl3)
δ 167.37, 147.87, 146.73, 144.60, 127.07, 123.04, 115.70, 114.68,
109.27, 77.22, 77.01, 76.80, 64.62, 60.40, 55.94, 31.93, 29.70, 29.69,
29.66, 29.61, 29.56, 29.37, 29.32, 28.78, 26.01, 22.70, 14.13.
f1 (ppm)

MS^1(447.42)

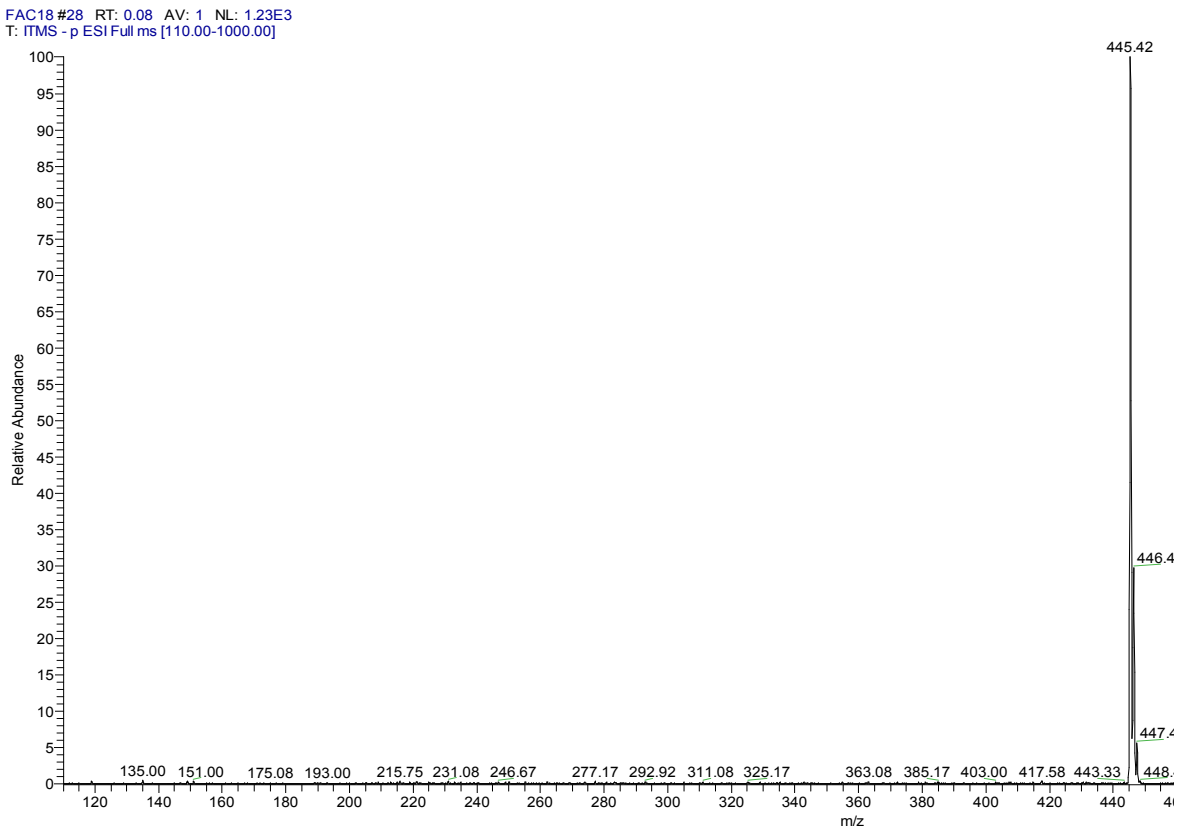
FAC18 #28 RT: 0.08 AV: 1 NL: 1.23E3
T: ITMS - p ESI Full ms [110.00-1000.00]
445.42
446.4
Relative Abundance
m/z
135.00 151.00 175.08 193.00 215.75 231.08 246.67 277.17 292.92 311.08 325.17 363.08 385.17 403.00 417.58 443.33

MS^2

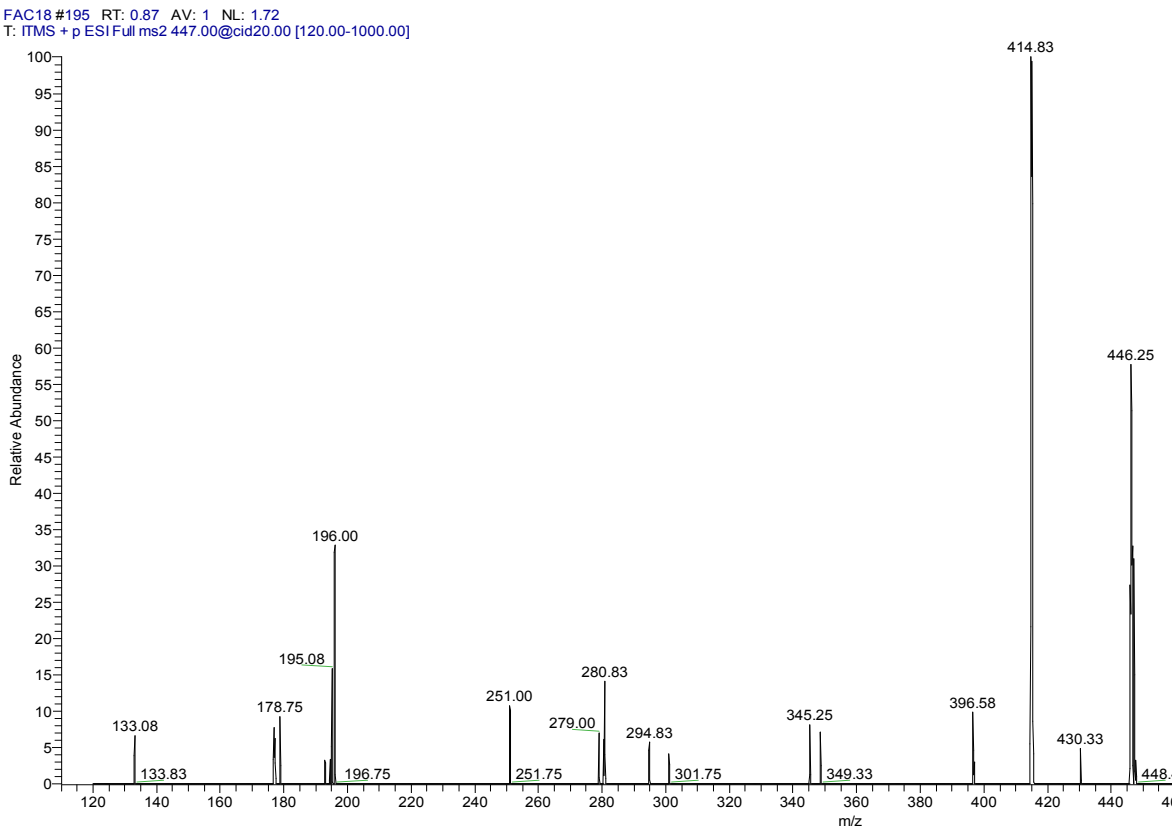

The purity of our products (FAEs) prepared in our laboratory can meet the requirements for the identification of their molecular structure through nuclear magnetic resonance (NMR). And the purity of FAEs is better than 98% (HPLC grade). More detailed data have been shown blow.

FAC2 (100%, HPLC)

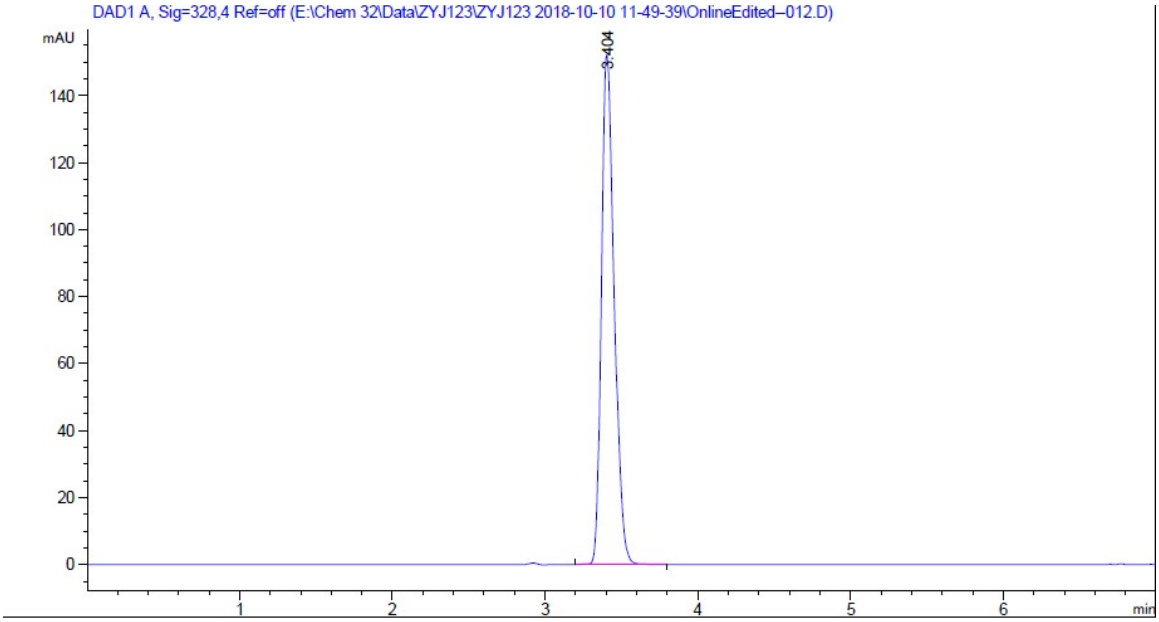

Retention time peak area

峰 #	保留时间 [min]	类型	峰宽 [min]	峰面积 [mAU*s]	峰高 [mAU]	峰面积 %
1	3.404	BB	0.0875	882.25348	152.45941	100.0000

FAC4 (98.79%, HPLC)

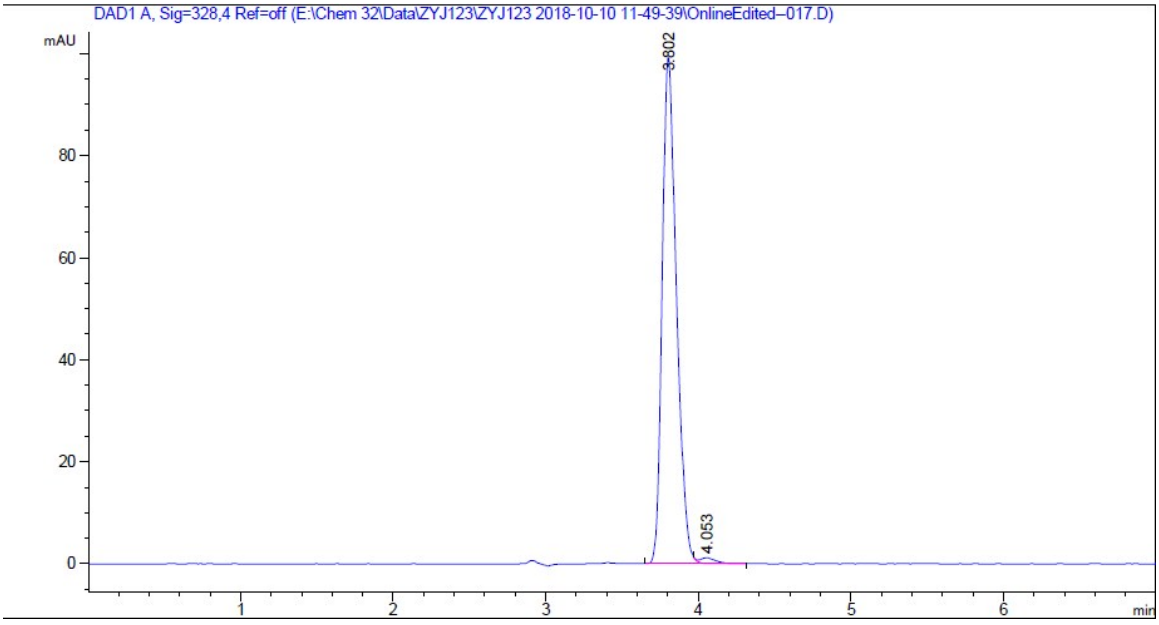

Retention time peak area

峰 #	保留时间 [min]	类型	峰宽 [min]	峰面积 [mAU*s]	峰高 [mAU]	峰面积 %
1	3.802	BV R	0.0976	644.64685	99.52769	98.7954
2	4.053	VB E	0.1006	7.85981	1.13820	1.2046

FAC6 (100%, HPLC)

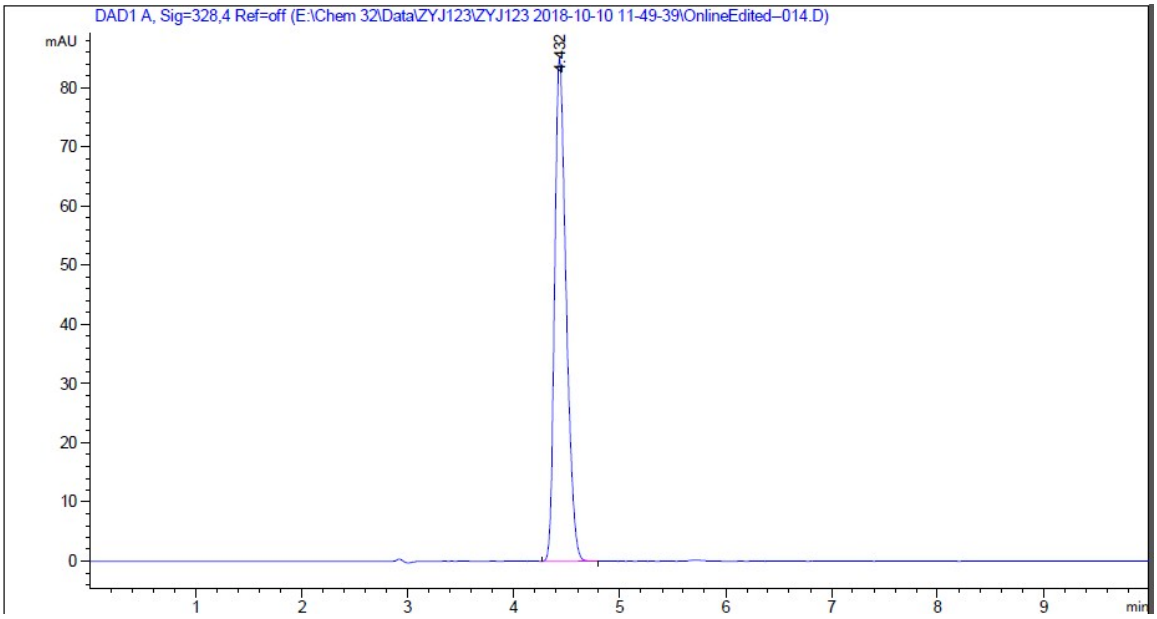

Retention time peak area

峰 #	保留时间 [min]	类型	峰宽 [min]	峰面积 [mAU*s]	峰高 [mAU]	峰面积 %
1	4.432	BB	0.1137	640.10791	85.15678	100.0000

FAC8 (100%, HPLC)

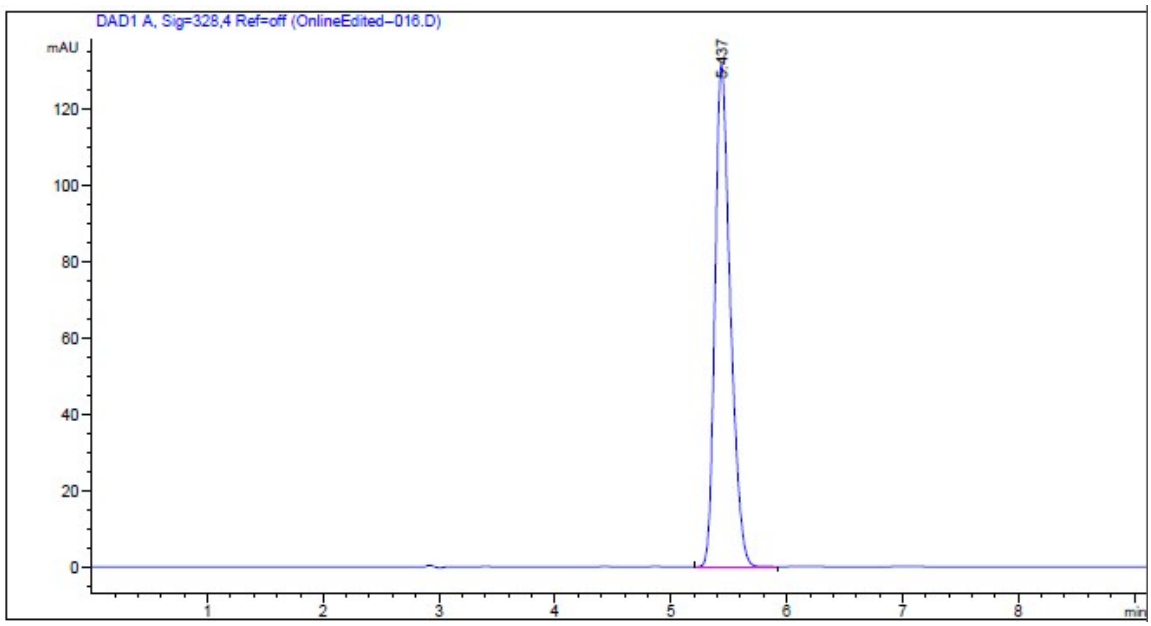

Retention time peak area

峰 #	保留时间 [min]	类型	峰宽 [min]	峰面积 [mAU*s]	峰高 [mAU]	峰面积 %
1	5.437	BB	0.1375	1213.82275	131.74413	100.0000

FAC10 (100%, HPLC)

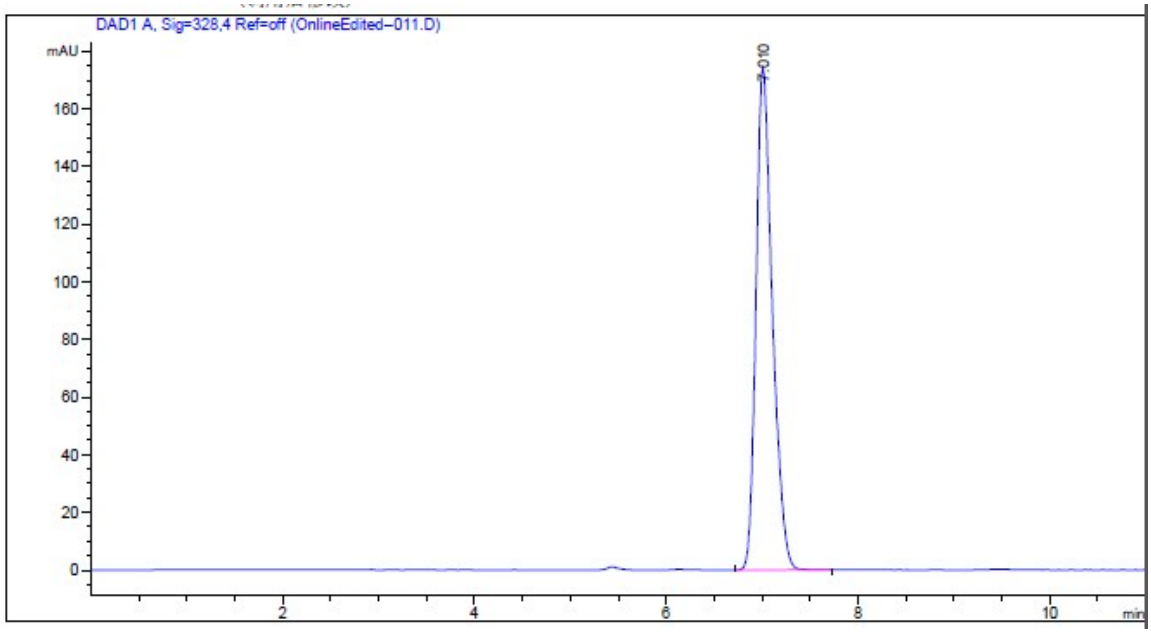

Retention time peak area

峰 #	保留时间 [min]	类型	峰宽 [min]	峰面积 [mAU*s]	峰高 [mAU]	峰面积 %
1	7.010	BB	0.1785	2067.90332	174.19380	100.0000

FAC12 (100%, HPLC)

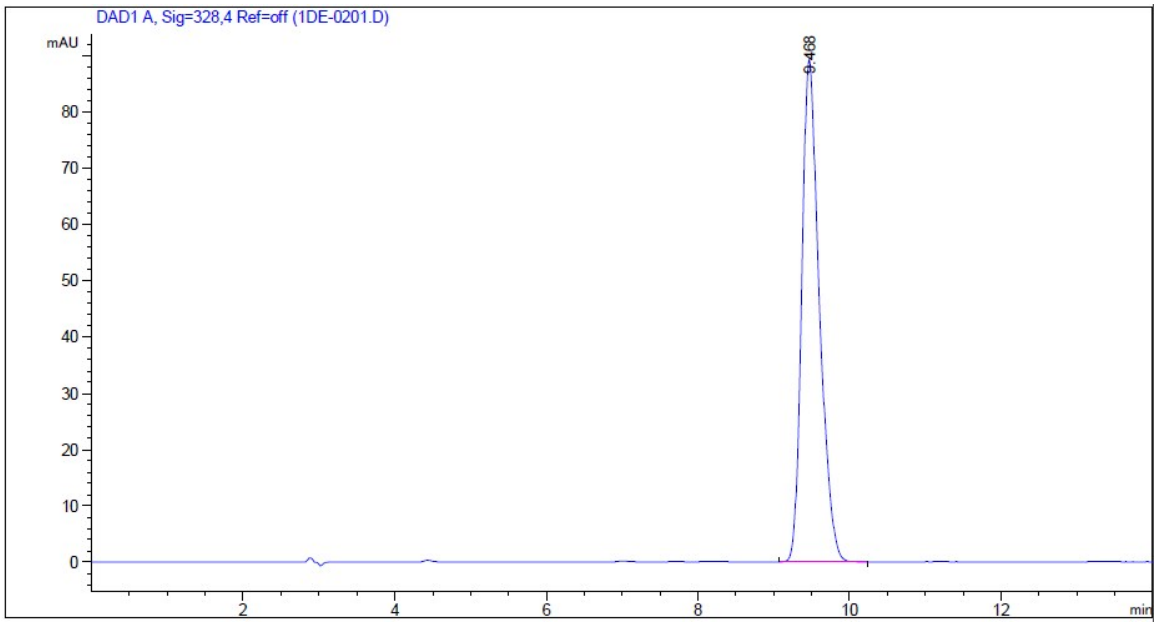

Retention time peak area

峰 #	保留时间 [min]	类型	峰宽 [min]	峰面积 [mAU*s]	峰高 [mAU]	峰面积 %
1	9.468	BB	0.2401	1439.49011	89.25983	100.0000

FAC14 (100%, HPLC)

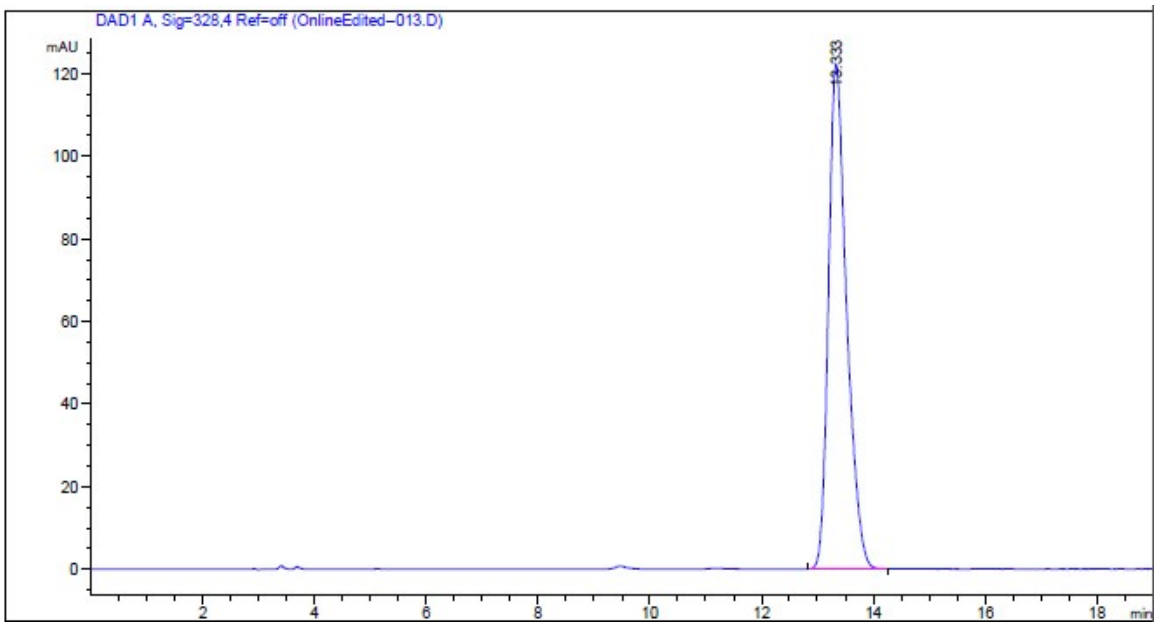

Retention time peak area

峰 #	保留时间 [min]	类型	峰宽 [min]	峰面积 [mAU*s]	峰高 [mAU]	峰面积 %
1	13.333	BB	0.3369	2753.63354	122.21925	100.0000

FAC16 (95.8%, HPLC)

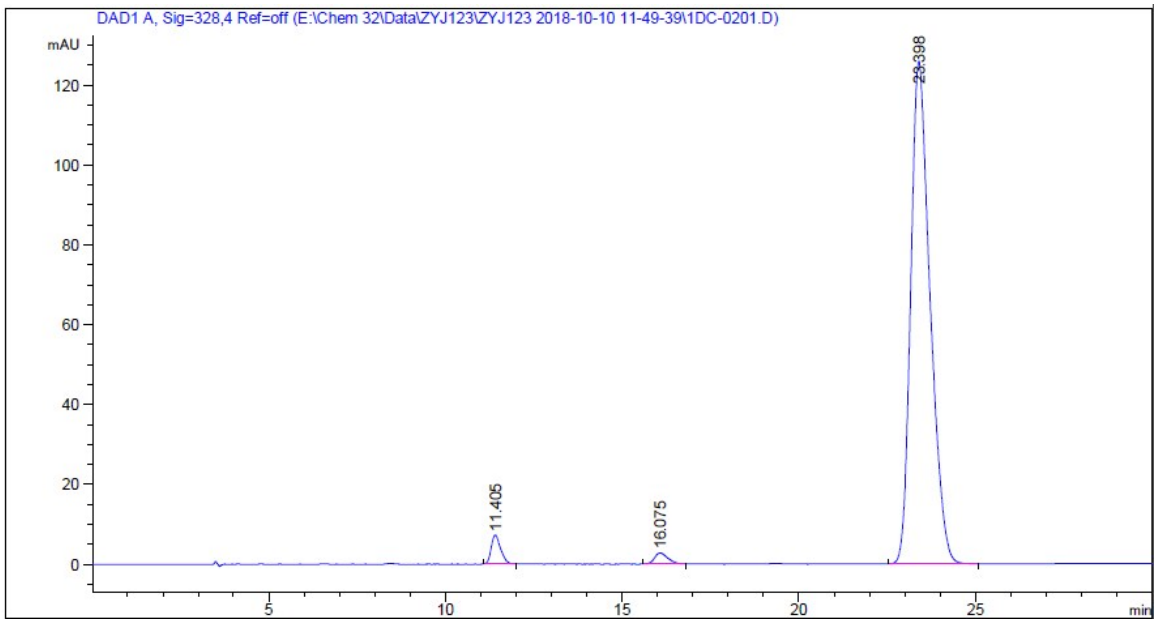

Retention time peak area

峰 #	保留时间 [min]	类型	峰宽 [min]	峰面积 [mAU*s]	峰高 [mAU]	峰面积 %
1	11.405	BB	0.2747	135.44350	7.29204	2.7107
2	16.075	BB	0.3768	74.09706	2.83594	1.4829
3	23.398	BB	0.5636	4787.11914	125.90565	95.8064

FAC18 (99.8%, HPLC)

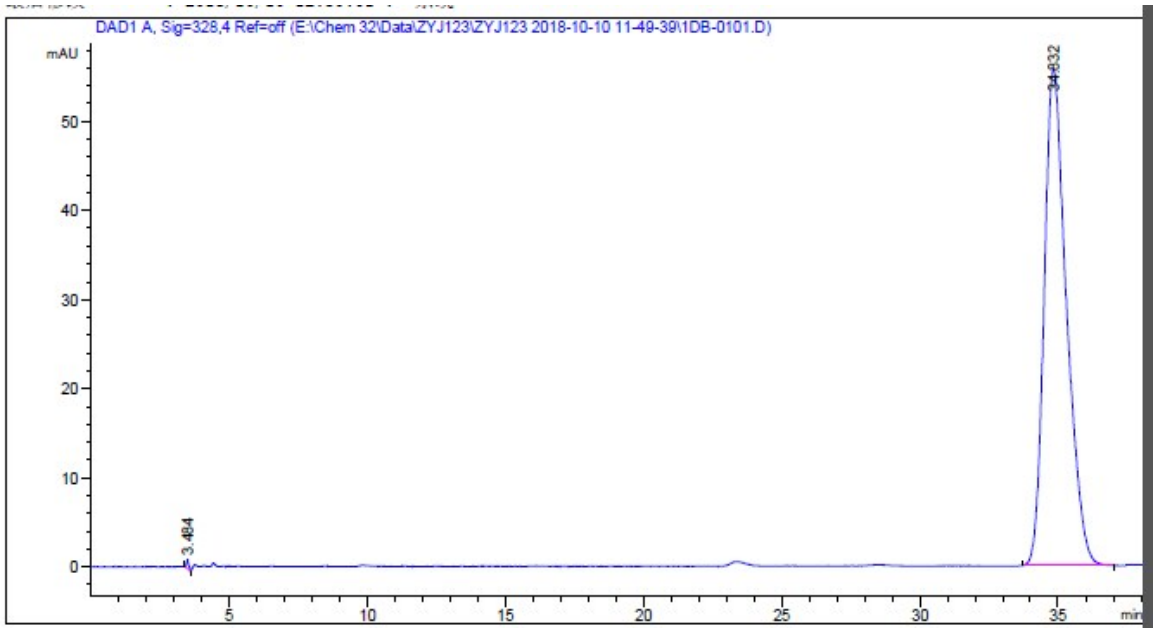

Retention time peak area

峰 #	保留时间 [min]	类型	峰宽 [min]	峰面积 [mAU*s]	峰高 [mAU]	峰面积 %
1	3.484	BB	0.0782	5.49889	1.03201	0.1755
2	34.832	BB	0.8254	3128.35864	55.68715	99.8245